AtSnRK2.4 Functions as an ABA-Responsive Protein Kinase in Arabidopsis

Mattia Adamo, Colette Tournaire-Roux, Valérie Rofidal, Philippe Nacry, Vincent Demolombe - Liozu, Amandine Crabos, Christophe Maurel, Véronique Santoni

Physiologia Plantarum

ORIGINAL RESEARCH OPEN ACCESS

*At*SnRK2.4 Functions as an ABA-Responsive Protein Kinase in Arabidopsis

Mattia Adamo | Colette Tournaire-Roux | Valérie Rofidal | Philippe Nacry | Vincent Demolombe | Amandine Crabos | Christophe Maurel | Véronique Santoni

Institute for Plant Sciences of Montpellier, University Montpellier, CNRS, INRAE, Institut Agro, Montpellier, France

Correspondence: Christophe Maurel (christophe.maurel@cnrs.fr) | Véronique Santoni (veronique.santoni@inrae.fr)

Received: 27 May 2025 | **Revised:** 8 September 2025 | **Accepted:** 16 September 2025

Handling Editor: R.M. Rivero

Funding: This work was supported by a grant from the Agence Nationale de la Recherche (ANR-18-CE92-0055-01).

Keywords: abscisic acid | phospho-proteomics | protein kinase | root development | signaling | SnRK2.4

ABSTRACT

In *Arabidopsis*, members of subclasses I and III of sucrose non-fermenting 1-related subfamily protein kinases 2 (SnRK2) are considered to be mainly osmotic- and ABA-responsive, respectively. In this work, we report on the role of SnRK2.4, a member of subclass I, in shaping plant root architecture (e.g., lateral root growth and root primordia emergence) in response to exogenous ABA. We show that SnRK2.4 is active in standard conditions and upon ABA treatment, with a higher ABA sensitivity than SnRK2.2 and SnRK2.3 from class III. To identify the molecular substrates of SnRK2.4, we compared the transcriptome, proteome, and phosphoproteome of wild-type and *snrk2.4* plants, in standard conditions and after a 1 μM ABA treatment. The phosphoproteomic analysis, which relies on 3858 unique phosphopeptides corresponding to 1820 phosphoproteins, revealed that 186 and 277 proteins were under-phosphorylated in *snrk2.4* mutants, in control conditions and upon ABA treatment, respectively. A regulation by SnRK2.4 of membrane transporters and cell-to-cell communication was highlighted in both conditions. By contrast, in response to ABA, SnRK2.4 specifically induced a decreased abundance of RNA helicases, suggesting that SnRK2.4 can interfere with mRNA splicing. SnRK2.4 also modulated the phosphorylation of proteins putatively involved in attenuation of ABA signaling, in lipid signaling, and in cellulose biosynthesis, via a complex PK cascade involving mainly calcium-dependent PKs. This work shows that SnRK2.4 is an ABA-responsive SnRK2, with high hormone sensitivity and putative roles in fundamental aspects of cell physiology.

1 | Introduction

The phytohormone abscisic acid (ABA) coordinates plant growth and development as well as responses to stressful environments, in particular drought stress. ABA mediates rapid cellular responses such as transcriptional and metabolic reprogramming, along with long-term developmental adjustments of the entire plant (Cutler et al. 2010). The core of ABA perception comprises receptor proteins of the PYRABACTIN RESISTANCE1 (PYR1)/PYR1-LIKE (PYL)/REGULATORY COMPONENTS OF ABA RECEPTORS (RCAR) class, clade A protein phosphatases 2C (PP2C) working as co-receptors, and sucrose non-fermenting 1-related subfamily protein kinases 2 (SnRK2). SnRK2s form a family with 10 members (SnRK2.1-2.10) in *Arabidopsis thaliana* (Kamiyama, Katagiri, and Umezawa 2021) classified into three classes (I–III). Among SnRK2s, members of class III (SnRK2.2, 2.3, 2.6) are considered the main positive regulators of ABA signaling. In the absence of the hormone, these SnRK2s are kept in an inactive, dephosphorylated state by the interaction with PP2Cs. When ABA levels rise, the hormone forms ternary

complexes with PYR1/PYL/RCAR and PP2C, releasing SnRK2s from inhibition (Chen et al. 2020; Cutler et al. 2010), thereby allowing SnRK2-mediated phosphorylation and regulation of downstream targets (Chen et al. 2020; Soon et al. 2012).

SnRK2s have long been identified as central players in plant hormonal and environmental stress signaling (Fujii et al. 2011; Kulik et al. 2011). Although responsive to both ABA and osmotic stress, SnRK2s from class III were proposed to act as the main regulators of ABA signaling, whereas class I would be exclusively responsive to osmotic stress (Boudsocq et al. 2004; Soma et al. 2021). Strikingly, knock-out mutations of all class III SnRK2s induce dramatic phenotypes showing little or no responses to high ABA concentrations during seed germination, root growth, and stomatal movement (Fujii and Zhu 2009). The regulation of class III SnRK2s was described to occur through transphosphorylation by Raf-like protein kinases (RAFs) (Kamiyama, Katagiri, and Umezawa 2021; Lin et al. 2021; Takahashi et al. 2020). Class III SnRK2s, in turn, activate downstream targets including several transcription factors, such as ABRE-BINDING PROTEINS (AREBs)/ABRE-BINDING FACTORS (ABFs), which in turn induce the expression of ABA-responsive genes (Chen et al. 2020; Cutler et al. 2010).

On the other hand, class I SnRK2s (SnRK2.1, 2.4, 2.5, 2.9, 2.10) have been generally considered as ABA-unresponsive (Boudsocq et al. 2004; Fujii et al. 2011) and rather respond to salinity and osmotic stress (McLoughlin et al. 2012). Subclass I SnRK2s regulate proteins involved in mRNA decay, in particular VARICOSE, to adjust transcriptional stability and mediate plant growth under drought and salinity stress in an ABA-independent pathway (Fàbregas et al. 2020; Kawa et al. 2020; McLoughlin et al. 2012; Soma et al. 2017). Yet, heterologous expression studies in yeast aiming to test the functionality of a variety of core ABA signaling components indicated that SnRK2.4 may be involved in ABA-dependent signaling (Ruschhaupt et al. 2019). In support of this, a recent study revealed the role of SnRK2.4 in ABA-dependent downregulation of root aquaporin activity and consequent reduction of water transport to aerial parts (Shahzad et al. 2024). SnRK2.4 and SnRK2.10, which belong to the same SnRK2 class, have been previously found to be activated by salt and hyperosmotic stress in Arabidopsis roots (McLoughlin et al. 2012) or when transiently expressed in cell culture protoplasts (Boudsocq et al. 2004). SnRK2.4 and SnRK2.10 were also shown to regulate root growth and architecture in saline conditions (McLoughlin et al. 2012). In addition, salt stress induced a rapid re-localization of SnRK2.4 from the cytosol to punctate structures in root cells, putatively through the binding of phosphatidic acid (PA) (McLoughlin et al. 2012). A specific binding of both SnRK2.10 and SnRK2.4 to PA-containing liposomes was demonstrated (McLoughlin et al. 2012), and SnRK2.10 was identified in a proteomics screen for its binding capacity to PA (Testerink et al. 2004).

Phosphoproteomics has been used as a powerful approach to investigate functions targeted by protein kinases (PK). For instance, phosphoproteomics analyses of double *snrk2.2x2.3* and triple *snrk2* mutants lacking all subclass III SnRK2s have been performed to investigate SnRK2-mediated phosphorylation signaling (Umezawa et al. 2013; Wang et al. 2013). Mitogen-activated PK (MPK) 1, MPK2, SnRK2 substrate 1 (SNS1), and bZIP transcription factors, including AREB1/ABF2, AREB3, and ENHANCED EM LEVEL (EEL), were identified as candidate substrates of subclass III SnRK2s. Phosphoproteomics also pointed to the role of SnRK2.2 and SnRK2.3 in flowering time regulation, nucleic acid binding, miRNA and epigenetic regulation, signal transduction, as well as chloroplastic functions (Umezawa et al. 2013, Wang et al. 2013). Recently, a novel phosphoproteomic approach (KALIP2.0 method) was reported to integrate in vivo and in vitro information and thereby identify the direct targets of PKs (Wang et al. 2020). The results showed that ABA-stimulated SnRK2.6 and osmotically activated SnRK2.4 differed in their targets, confirming the strength of such an approach in detecting PK specificity. However, these physiological characterizations of SnRK2 mutants have remained incomplete. Consequently, the individual or combined contributions of SnRK2s to the variety of ABA responses *in planta* are still unclear.

The present study addresses the responses of SnRK2.4 to ABA with regard to root development and membrane cellular functions. For this, we developed an integrated transcriptomic, proteomic, and phosphoproteomic study of *snrk2.4* knock-out mutants. SnRK2.4 appears as a true ABA-responsive SnRK2, putatively coordinating membrane transporters, interfering with cell-to-cell communication, RNA translation, cellulose biosynthesis, and lipid signaling.

2 | Materials and Methods

2.1 | Plant Materials and Growth Conditions

Arabidopsis thaliana ecotype Columbia (Col-0) was used as the control wild-type (WT) plant. The *snrk2.4-1* (Salk_080588) and *snrk2.4-2* (Salk_146522) single T-DNA insertion mutant alleles were obtained from Christa Testerink's laboratory (Wageningen University, The Netherlands). For proteomic and transcriptomic analyses, Col-0, *snrk2.4-1*, and *snrk2.4-2* seeds were surface sterilized and sown on solid 0.5 × Murashige and Skoog (MS) pH 5.8, 1% Agar. Seedlings were grown for 7 days under long day conditions (16/8 h light/dark) at a constant temperature of 21.5°C in a Fitoclima D1200 chamber (Aralab). After this time, seedlings were gently transferred to a Hoagland-based hydroponic solution (1.25 mM KNO_3, 1.50 mM $Ca(NO_3)_2$, 0.75 mM $MgSO_4$, 0.50 mM KH_2PO_4, 50 μM H_3BO_3, 12 μM $MnSO_4$, 0.70 μM $CuSO_4$, 1 μM $ZnSO_4$, 0.24 μM Na_2MoO_4, 50 μM Fe-EDTA, 100 μM Na_2SiO_3) and let grow for two additional weeks under the same photoperiod. The solution of the hydroponic cultures was replaced weekly. For ABA treatment, a stock solution of 100 mM was prepared in ethanol and diluted to a final concentration of 1 μM. Standard condition corresponds to a mock treatment with ethanol. Roots were collected and microsomal proteins were extracted freshly.

2.2 | Microsome Extraction

Root microsomal proteins were extracted according to (Di Pietro et al. 2013) with slight modifications. Microsomal pellets were suspended in a conservation buffer composed of 10 mM Tris-HCl pH 6.8, 250 mM sorbitol, 20% glycerol, 4.2 μM leupeptin,

1 mM pefabloc, 5 mM DTT, 5 mM beta-glycerol phosphate, 1 mM Na-vanadate, and 1:100 (v/v) Phosphatase Inhibitor Cocktail 2 (Sigma-Aldrich P5726), and 1:100 (v/v) Phosphatase Inhibitor Cocktail 3 (Sigma-Aldrich P0044).

2.3 | Root Architecture Analyses

Seeds were stratified for 2 days at 4°C and grown vertically on ½ MS pH 5.8, 1% Agar for 5 days under long day conditions (16/8 h light/dark) at a constant temperature of 21.5°C in a Fitoclima D1200 chamber (Aralab). After this time, seedlings were gently transferred onto plates containing the same medium supplemented with 1 or 5 μM ABA, or mock (ethanol), and were allowed to grow for 10 additional days. Plate images were taken with a 16 M pixel linear camera, a telecentric objective, and a collimated LED backlight (Vegeled Floodlight, Colasse Seraing, Belgium). Root length and LR numbers were both measured in the root zone formed after plant transfer using the ImageJ software (Schneider et al. 2012). To measure primordia density, roots were cut and stored in 70% ethanol. Primordia were counted with an Olympus BX61 microscope until the emergence of the first lateral root, and their number was reported as the distance between the root tip and the first lateral root.

2.4 | Gene Expression

Total RNAs were isolated using an SV RNA isolation kit (Promega) and treated with RQ1 DNAse (1 U μg^{-1} RNA) at 37°C for 1 h. Each sample was a pool of 5–6 plants. RNAs were quantified with a NanoDrop ND-1000 spectrophotometer (Thermo Fischer Scientific), and data quality was checked using a non-denaturing gel electrophoresis. For quantitative reverse transcription polymerase chain reaction (qRT-PCR) analyses, 2 μg of total RNA were used for cDNA synthesis, and qRT-PCR was performed as described (Shahzad et al. 2024). The transcript abundance was expressed relative to the expression of *UBC21* (At5g025760) transcripts in a Col-0 sample used as calibrator and, in all samples, relative to the average expression of *UBC21* (At5g025760) and *YSL8* (At5g08290) transcripts used as reference genes. The primer sequences used are described in Table S1 and in (Czechowski et al. 2005). Three biological replicates and two technical repeats per replicate were used. ANOVA analysis followed by post hoc Tukey test was used to assess statistical differences. For microarray analysis, 100 ng of total RNA of each sample were amplified using the GeneChip WT PLUS Reagent Kit (Affymetrix) following the manufacturer's instructions. Labeling and hybridization were carried out as described in (Shahzad et al. 2016). For microarray analyses, the transcript abundance between samples was evaluated as significantly different by a Student *t*-test using 3 independent biological replicates/genotype. $p < 0.05$ was considered statistically significant. The transcriptomics data were deposited at EBI with identifier E-MTAB-15518.

2.5 | Protein Digestion

For proteome and phospho-proteome analyses, 3 independent biological replicates for all 6 conditions (WT plant, *snrk2.4-1* and *snrk2.4-2* mutants, in control conditions, and upon 1 μM ABA) were obtained, and a fourth replicate was built with an equal mixture of the 3 biological repeats. One hundred micrograms-microsomes were fractionated using precast 10% SDS-PAGE gel electrophoresis (Biorad). Gels were stained with Blue-G colloidal. Each lane was cut into 3 bands. Gel slices were treated according to (Chen, Rofidal, et al. 2019). Proteins were digested with trypsin (Sequencing Grade Modified Trypsin, Promega) at a 1:50 (trypsin: protein) ratio at 37°C overnight. Peptides were obtained and treated according to (Chen, Rofidal, et al. 2019). 5% of the sample was used for total proteome analysis, and the remaining sample was used for phosphoproteome analysis. The samples were dried in a concentrator centrifuge under vacuum and resuspended in 10 μL of 2% fluoric acid (FA) for proteome analysis and in 30 μL loading buffer A [5% trifluoroacetic acid (TFA) in 80% acetonitrile (ACN)] for phosphoproteome analysis.

2.6 | Phospho-Peptide Enrichment

Titane sphere TiO_2 (5 μm, Interchim, Montluçon) resuspended in isopropanol at a concentration of 48 $\mu g\,\mu l^{-1}$, was packed at the bottom of a tip. Two titanium columns made of 300 and 600 μg of TiO_2 beads each were centrifuged at 100 *g* for 3 min and at 400 *g* for 10 min to get rid of isopropanol and were stacked. Beads were washed with 20 μL of buffer B (1% TFA in 80% ACN) and equilibrated twice with 20 μL buffer A. The peptide sample was loaded by centrifugation at 90 *g* for 3 min and then at 360 *g* for 20 min on the 2 columns. After loading, each column was washed with 20 μL buffer A and then with 20 μL of buffer B twice. Peptides were eluted successively with 10 μL of 0.5% NH_4OH, 10 μL of 5% NH_4OH, and finally with 10 μL of 5% NH_4OH in 20% ACN. Titanium eluates were combined and acidified with 30 μL of 100% FA before being dried in a concentrator centrifuge under vacuum and resuspended in 8 μL of 2% FA. The flow through of both titanium columns was collected, pooled, and evaporated before being resuspended in 10 μL of 2% FA.

2.7 | LC–MS/MS Analysis

The LC–MS/MS experiment was performed with an Ultimate 3000 RSLC nano system (Thermo Fisher Scientific Inc.) interfaced online with a nano easy ion source and an Exploris 240 Orbitrap mass spectrometer (Thermo Fisher Scientific Inc.). The samples were analyzed in a Data Dependent Acquisition (DDA) mode. Peptides were first loaded onto a pre-column (Thermo Scientific PepMap 100 C18, 5 μm particle size, 100 Å pore size, 300 μm i.d. × 5 mm length) from the Ultimate 3000 autosampler with 0.05% TFA in water at a 10 μL min^{-1} flow rate. The peptides were separated by reverse-phase column (Thermo Scientific PepMap C18, 2 μm particle size, 100 Å pore size, 75 μm i.d. 50 cm length) at a 300 nL min^{-1} flow rate. After a 3 min loading period, the column valve was switched to allow elution of the peptides from the pre-column onto the analytical column. The loading buffer (solvent A) was 0.1% FA in water, and the elution buffer (solvent B) was 0.1% FA in 80% ACN. The linear gradient was 2%–25% of solvent B in 103 min, then 25%–40% of solvent B from 103 to 123 min, and finally 40%–90% of solvent B from 123 to 125 min. The total run time was 150 min, including a high organic wash step and a re-equilibration step. Peptides were transferred to the gaseous phase with positive ion electrospray ionization at 1.9 kV. In DDA,

the top 15 precursors were acquired between 270 and 1200 m/z with a 2th (Thomson) selection window, dynamic exclusion of 40 s, normalized collision energy (NCE) of 30, and resolutions of 120,000 for MS and 15,000 for MS2. Spectra were recorded with the Xcalibur software (4.7.69.37) (Thermo Fisher Scientific). The mass spectrometry data were deposited to the ProteomeXchange Consortium via the PRIDE partner repository with the dataset identifier PXD061019.

2.8 | Identification and Quantification of the Whole Proteome and Phosphoproteome

The resulting mass spectrometry data were processed using MaxQuant with an integrated Andromeda search engine (version 2.2.0.0). Tandem mass spectra were searched against the Araport11 database (48,359 entries). The minimal peptide length was set to 5. The criterion "Trypsin/P" was chosen as the digestion enzyme. The carbamidomethylation of cysteine was selected as a fixed modification, and methionine oxidation and N-terminal acetylation were systematically selected as variable modifications. Up to 2 missed cleavages were allowed. The function "Match between run" was used. For total proteome analysis, proteins were identified from at least two tryptic peptides, including a unique peptide. The rate of false peptide sequence assignment and false protein identification was fixed to be lower than 1%. Peptide ion intensity values derived from MaxQuant were subjected to label-free quantitation (LFQ). To investigate differentially expressed proteins, a Student's *t*-test was performed using protein LFQ intensity values. For phosphoproteome analysis, the variable modification "phosphorylation at S, T, and Y" was additionally considered, and a phosphopeptide was qualified provided a minimal score of 40 in at least one biological repeat. To normalize samples, the intensity of each peptide from the "evidence" table was reported to the sum of all peptides' intensity in each sample (Figure S1). The phosphopeptide abundance between samples was evaluated as significantly different by a Student *t*-test. $p < 0.05$ was considered statistically significant.

2.9 | Bioinformatic Analyses

Gene Ontology (GO) was used to test gene lists for biological process, molecular function, and cellular component enrichment using Panther 19.0 (http://www.pantherdb.org/) (Mi et al. 2013). The p-logo software (https://plogo.uconn.edu/) was used to analyze the models of the sequences with amino acids in specific positions of phosphorylated-21-mers (10 amino acids upstream and downstream of the phosphorylated site) in all of the protein sequences. The Arabidopsis proteome was used as the background database, and the other parameters were set to default values.

3 | Results

3.1 | SnRK2.4 Regulates Lateral Root Density

The effects of ABA on root development are diverse, acting primarily on primary root growth and lateral root density (LRd). To evaluate the roles of SnRK2.4 in root growth responses to ABA, we compared these two traits in WT plants (Col-0), in two independent *snrk2.4* insertional mutants, and in a *snrk2.2xsnrk2.3* double mutant, under standard conditions and upon ABA treatment. The *snrk2.2xsnrk2.3* genotype was included as a reference because of its well-established ABA insensitivity (Fujii and Zhu 2009).

Five-day-old seedlings were transferred to ½ MS medium (Murashige and Skoog 1962), either standard or supplemented with 1 or 5 μM ABA. Plants were then allowed to vertically grow for 10 days, and the incremental growth of the primary root as well as the newly formed LRs was computed (Figure S3). The calculation of LRs number (Table S2.2) and the normalization of LRs number to the primary root length (Table S2.3) gave similar ABA inhibition, suggesting that the effect of ABA on primary root length is negligible compared to its effect on primordia development. We further considered primary root length as well as LRs and primordia densities (Figures 1 and 2). In standard conditions, we observed that all mutants exhibited, with respect to WT, a reduced primary root length and LRd (Figure 1A), suggesting that SnRK2.2, 2.3, and 2.4 can promote root growth and branching. However, ABA treatment revealed contrasted behaviors among mutants: in the presence of 5 μM ABA, a primary root growth inhibition of around 25% was observed in the WT and *snrk2.4* genotypes, while the root growth of the double mutant *snrk2.2xsnrk2.3* was unaltered (Figure 1A). Thus, SnRK2.2 and/or SnRK2.3 are the main positive regulators of ABA-mediated repression of primary root growth in response to high ABA dose (i.e., 5 μM).

As reported in earlier studies, Arabidopsis primary and lateral roots exhibit different sensitivities to ABA-mediated growth inhibition, the lateral roots being noticeably more sensitive than the primary root (De Smet et al. 2003). Accordingly, while the primary root growth was not affected, we observed a net reduction of LRd by 18% in WT plants when grown in the presence of 1 μM ABA (Figure 1B). Strikingly, a similar level of inhibition (21%) was observed in the *snrk2.2xsnrk2.3* double mutant, but not in the *snrk2.4* single mutants, the LRd of which was essentially insensitive to 1 μM ABA (Figure 1B). Upon exposure to 5 μM ABA, LRd inhibition was the strongest in WT plants (60%), somewhat lower in *snrk2.4* mutants (44%), and even more reduced in the *snrk2.2xsnrk2.3* mutant (31%) (Figure 1B). Interestingly, when compared to 1 μM ABA, the percentage of LRd inhibition at 5 μM ABA was almost identical in WT plants (51%) and *snrk2.4* mutants (43%), while not significantly different in the *snrk2.2xsnrk2.3* mutant (Figure 1B). These results indicate that SnRK2.4 is involved in shaping root architecture in response to low ABA concentrations (i.e., 1 μM) through inhibition of LRd. At higher ABA doses (i.e., 5 μM), SnRK2.2 and SnRK2.3 play a more prominent role, surpassing the action of SnRK2.4.

Because SnRK2.4 was rather sensitive to low exogenous ABA, we wondered whether such sensitivity was already noticeable at earlier developmental stages. For that, we used the same experimental set-up as described above and compared the density of lateral root primordia, all developmental stages being combined (Casimiro et al. 2003) between WT and *snrk2.4* genotypes, in the absence or presence of 1 or 5 μM ABA. We observed that 1 μM ABA induced a 58% inhibition of primordia density in the WT, while both *snrk2.4* genotypes were insensitive to 1 μM ABA

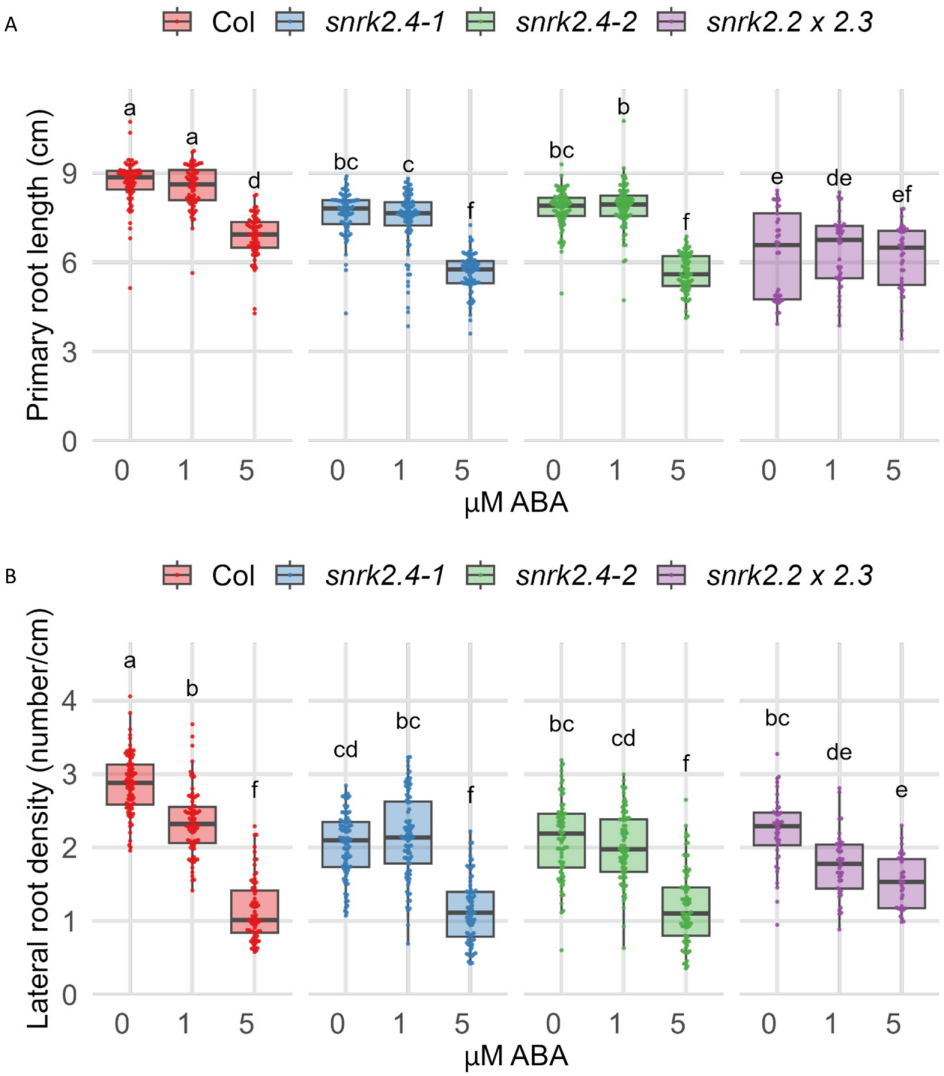

FIGURE 1 | Primary root length (A) and lateral root density (B) of WT plants (Col), *snrk2.4–1*, *snrk2.4–2*, and *snrk2.2xsnrk2.3* mutants grown in standard conditions or in the presence of 1 or 5 μM ABA. Plants were grown for 5 days in ½ MS medium and then transferred to ½ MS medium with the indicated ABA concentration. Root length and LR numbers were both measured in the root zone formed after plant transfer. Letters indicate a *p*-value below 0.05 from ANOVA pairwise comparisons using the Tukey HSD test. Numbers of plants are 81 (Col Ctr), 78 (Col 1 μM ABA), 70 (Col 5 μM ABA), 87 (*snrk2.4–1* Ctr), 84 (*snrk2.4–1* 1 μM ABA), 76 (*snrk2.4–1* 5 μM ABA), 71 (*snrk2.4–2* Ctr), 77 (*snrk2.4–2* 1 μM ABA), 73 (*snrk2.4–2* 5 μM ABA), 41 (*snrk2.2x2.3* Ctr), 40 (*snrk2.2x2.3* 1 μM ABA), 35 (*snrk2.2x2.3* 5 μM ABA).

(Figure 2). Noticeably, 5 μM ABA inhibited primordia formation in all genotypes (Figure 2).

The overall data indicate that SnRK2.4, on the one hand, and combined SnRK2.2 and SnRK2.3, on the other hand, respond to distinct concentration thresholds of ABA *in planta*, with SnRK2.4 showing a higher ABA sensitivity than SnRK2.2 and/or SnRK2.3.

3.2 | One μM ABA Alters Gene Expression and Protein and Phospho-Protein Abundance in WT Plants

The response of the Arabidopsis proteome to exogenous ABA has classically been studied using high ABA concentrations ranging from 50 to 100 μM ABA (El-Khatib et al. 2007; Kamiyama, Hirotani, et al. 2021; Kline et al. 2010; Umezawa et al. 2013; Wang et al. 2013; Zhu et al. 2017). However, mounting physiological evidence indicates that Arabidopsis roots can respond to much lower ABA concentrations (Dietrich et al. 2017; Miao et al. 2021). Moreover, we recently reported a clear reduction of hydraulic conductivity (Lp_r) of Arabidopsis roots treated with 1 μM ABA (Shahzad et al. 2024). Whereas a 1 h-ABA treatment did not alter Lp_r of WT plants, a 30% and 37% Lp_r reduction was observed upon a 3 h- and 5 h-ABA treatment, respectively (Shahzad et al. 2024). By contrast, the Lp_r of *snrk2.4* was unchanged after 3 and 5 h of ABA treatment. We therefore decided to focus our study on root responses to 1 μM exogenous ABA, at the earliest distinctive time point (3 h), and investigated the hormonal effects at both transcriptomic and proteomic levels.

Transcriptome analysis of WT roots through a micro-array procedure (Table S3, Figure 3) revealed 862 differentially expressed genes upon exposure to 1 μM exogenous ABA, of which 450 and 412 showed increased and decreased expression, respectively

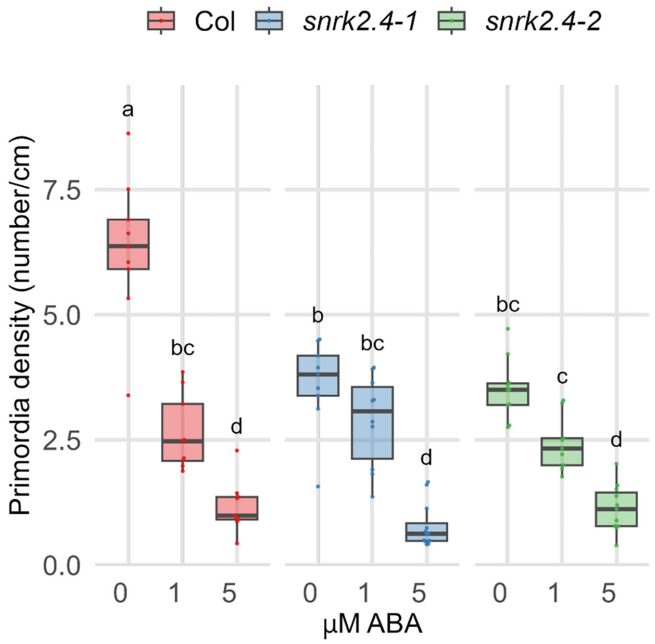

FIGURE 2 | Primordia density of WT plants (Col), *snrk2.4–1*, *snrk2.4–2*, and *snrk2.2xsnrk2.3* mutants grown in standard conditions or in the presence of 1 or 5 µM ABA. Plants were grown for 5 days in ½ MS medium and then transferred to ½ MS medium with the indicated ABA concentration. The number of primordia was measured in the root zone formed after plant transfer until the emergence of the first lateral root. Letters indicate a *p*-value below 0.05 from ANOVA pairwise comparisons using Tukey HSD test.

(Tables S3.2 and S3.3, Figure 3). Analysis of enriched GO terms revealed a striking overrepresentation of categories related to ABA response, protein dephosphorylation, and stimuli perception (Figure 3). Among the differentially expressed genes, all nine members of clade A PP2C phosphatases (Schweighofer et al. 2004) are induced by the ABA treatment (Table S3.2). Such an increase in PP2C expression, which was confirmed by quantitative RT-PCR (Figure 4), reflects a previously observed negative feedback loop mechanism to desensitize the ABA signaling pathway, thereby preventing plant cells from signal saturation (Fuchs et al. 2013).

To identify proteins and phosphoproteins that respond to ABA and to maximize the chances of identifying phosphorylation events associated with signal perception and responses, we decided to analyze a root microsomal fraction (Figure S2). While being highly enriched in membrane proteins, this fraction also contains significant amounts of soluble proteins (Berger et al. 2022). To increase the depth of analyses, microsomal proteins were fractionated into 3 bands by SDS-PAGE electrophoresis, and phosphopeptides were enriched using TiO_2 columns.

Using this pipeline, 7843 proteins (Table S4) were identified and quantified through at least two different tryptic peptides, with at least one being proteotypic to the protein under consideration. Compared to the standard condition, ABA treatment of WT plants induced the differential accumulation of 316 proteins, of which 115 and 201 were more or less accumulated, respectively (Figure 5, Tables S5.1, S5.2). By crossing our mass spectrometry data with corresponding transcriptome analysis, we observed that variations in protein abundance were generally not associated with changes in gene expression. Many over-accumulated proteins showed GO terms related to "response to ABA" as well as "response to water deprivation" (Figure 5B, Table S5.1), corroborating the idea that plants had properly perceived ABA in our experimental conditions. In addition, the less accumulated proteins showed an enrichment in GO terms associated with protein translation due to the reduced amount of several structural ribosomal proteins (Figure 5C, Table S5.2). This result supports previous observations indicating an inhibitory role of ABA on ribosome biogenesis (Guo et al. 2011).

By filtering the sequences of identified phosphopeptides with precise localization of phosphorylation sites and a MaxQuant score above 40, we could sort out 3858 phosphopeptides corresponding to 1820 proteins (Table S6, Figure S2). Their vast majority (91%) were found in a mono-phosphorylated state, with only 5%, 3.6%, and 0.4% as double, triple, and tetra phosphorylated, respectively (Table S6). Overall, the target phosphorylation residues were composed of 85% Ser, 12% Thr, and 3% Tyr residues (Figure S2).

To interpret phosphorylation changes, it is crucial to distinguish between a net variation in phosphorylation stoichiometry and mere changes in protein amount (Wu et al. 2011). For 97% of the retrieved phosphorylation events, we could not detect any variation in the corresponding protein amount, pointing to genuine up or down changes in protein phosphorylation. Upon ABA treatment, only 25 proteins showed decreased phosphorylation, whereas 151 proteins displayed increased phosphorylation (Table S5.3). A GO analysis showed that the latter proteins were mainly associated with root development, membrane transport, and PKs (Figure 6; Table S5.3). Among PKs, the calcium-dependent protein kinase (CDPK) family was overrepresented with 4 isoforms (CPK1, CPK6, CPK13, and CDPK-related kinase CRK2), confirming the close link between ABA and calcium signaling (Brandt et al. 2015; Diaz et al. 2016; Edel and Kudla 2016; You et al. 2023). The overall results show that the treatment of WT plants with 1 µM ABA for 3 h can induce changes in transcriptomic and proteomic profiles genuinely related to ABA signaling.

3.3 | *SnRK2.4* Mutation Reshapes the Phosphoproteome in Standard Conditions

Since *SnRK2.4* gene disruption induces a decrease in primary root growth, LRd (Figure 1) and root hydraulic conductivity (Shahzad et al. 2024) in plants grown in standard conditions, we wondered how SnRK2.4 can act on the transcriptome, proteome, and phosphoproteome in these conditions. Mutation of *SnRK2.4* in *snrk2.4-1* and *snrk2.4-2* plants induced consistent variations in the expression of 62 genes (Table S3.4) and in the abundance of 48 proteins, among which 18 proteins were down-accumulated and 30 were over-accumulated (Table S5.4). These results show that SnRK2.4 has a low impact on the transcriptome and proteome in standard conditions.

By contrast, the phosphorylation of 202 peptides corresponding to 185 proteins was significantly down-regulated in both *snrk2.4* mutants with respect to WT plants (Table S5.5). Among the 185

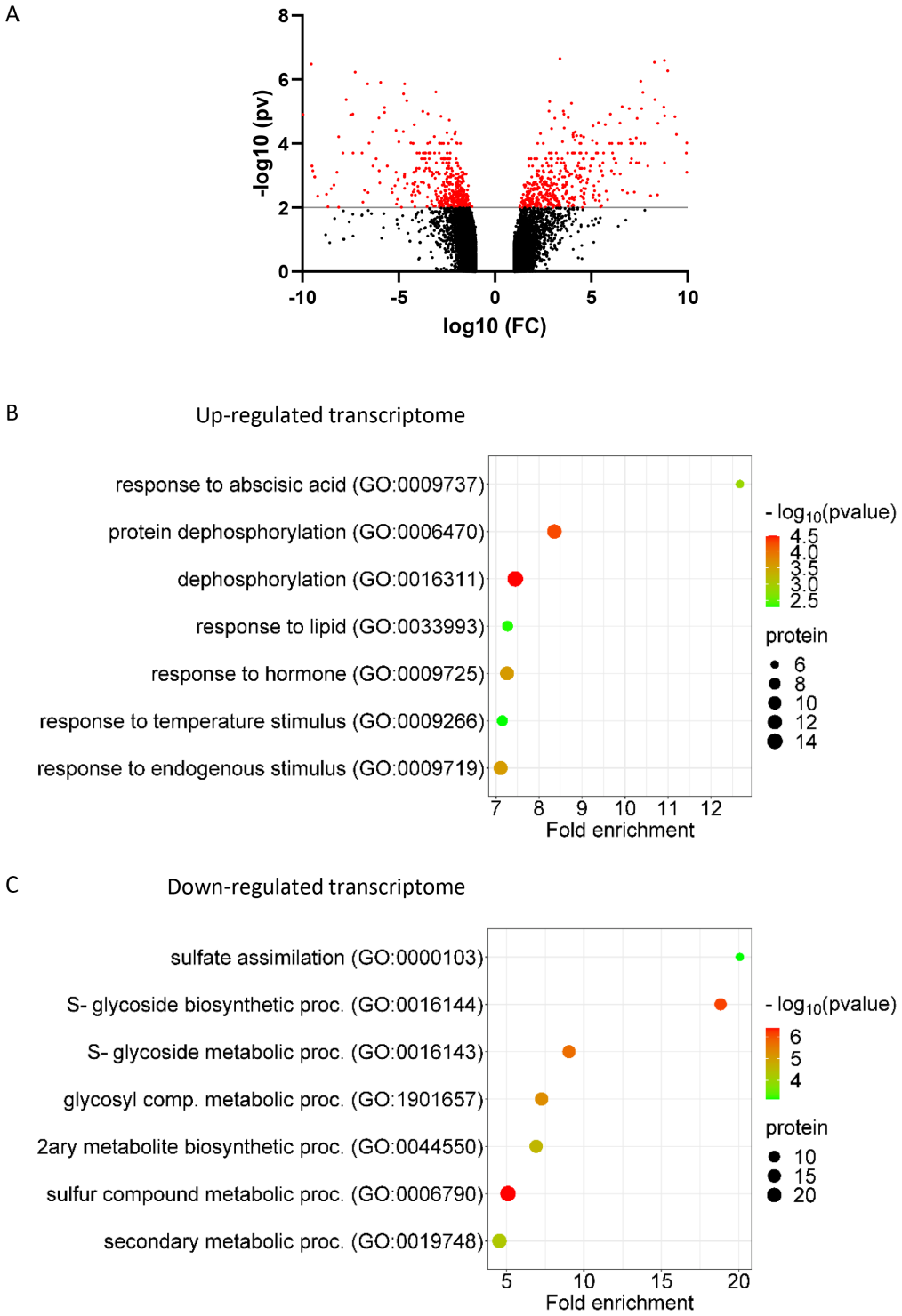

FIGURE 3 | Response of WT plant transcriptome to 1 μM ABA treatment for 3 h. (A) Volcano plot representing significant up- and down regulated gene expression in WT plants upon 1 μM ABA treatment. (B, C) Enriched biological process terms of up (B) and down (C) regulated gene expression. Significant corrected *p*-value and fold enrichment were below 10^{-3} and above 3, respectively. Genes characterizing each GO term are described in Table S3. proc., process.

proteins, 160 showed no variation in their abundance in both *snrk2.4* mutants. Thus, a large majority of phosphopeptide differences resulted from genuine differential phosphorylation events. This suggests that SnRK2.4 has a basal PK activity in the absence of any external stimulus, affecting directly or indirectly protein phosphorylation. The GO terms corresponding to the proteins with lower phosphorylation in *snrk2.4* plants were associated with transmembrane transport of nutrients (e.g., sucrose, nitrate, and potassium), ions (i.e., boron and calcium), and protons, plasmodesmata proteins, and PKs (Figure 7, Table S5.5). Hence, we could detect lower phosphorylation levels in 26 PKs, belonging to distinct PK families: receptor-like protein kinase (RLK), including leucine-rich (LRR) RLK (AT1G51800; AT1G51790; AT1G51890; AT3G02880.1; AT3G28450; AT4G20940; AT5G49770; LRK10L1),

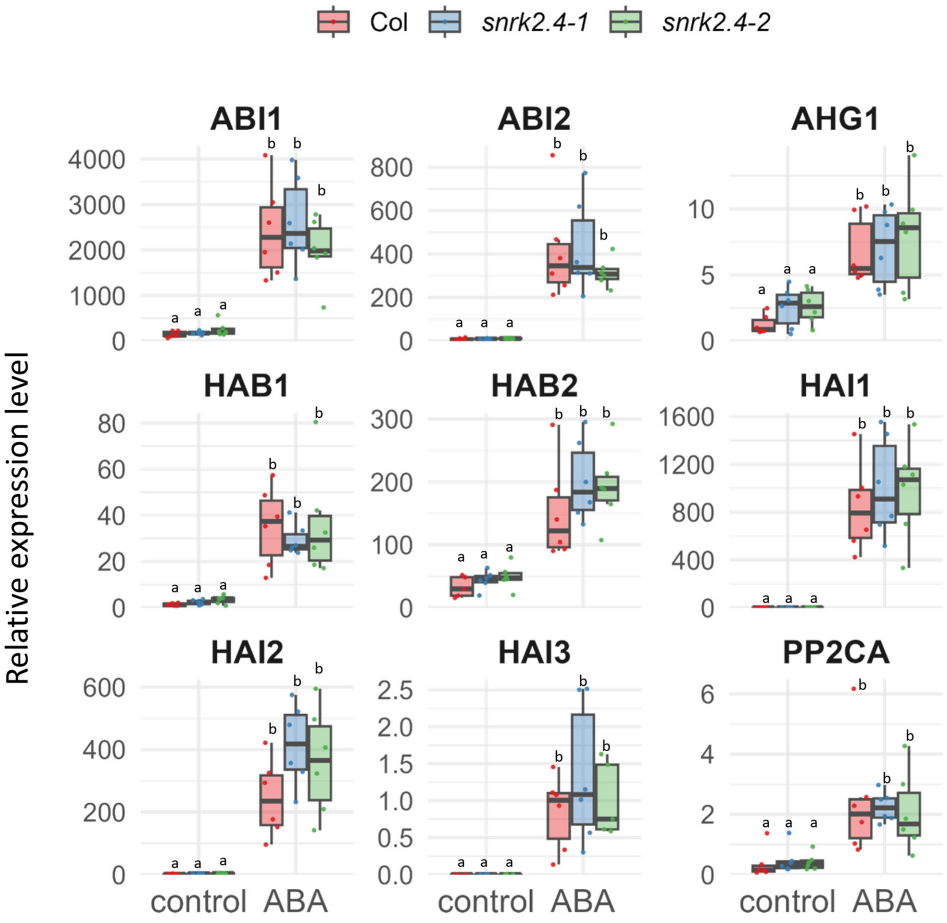

FIGURE 4 | Quantification of PP2C expression by Q-RT PCR. Q-RT PCR was performed as described in (Shahzad et al. 2024). The transcript abundance was expressed relatively to the expression of UBC21 (At5g025760) transcripts in a Col-0 sample used as calibrator and, in all samples, relatively to the average expression of UBC21 (At5g25760) and YSL8 (At5g08290) transcripts used as reference genes. Three biological replicates and two technical repeats per replicate were used. Letters indicate a *p*-value below 0.05 from ANOVA pairwise comparisons using Tukey HSD test.

MAPKs (M3KE1, MKK2, MPK16), cyclin-dependent kinase (CDGK2), and calcium-dependent PK (CDPK) (CPK7) (Table S5.5). Analysis of the phosphopeptides showing quantitative variations in *snrk2.4* mutants allowed us to identify 3 major motifs (Figure 8) that fit with the recognition sites of the PK families mentioned above. Thus, SnRK2.4 appears to be part of an extensive PKs cascade that, in standard conditions, acts on plasma membrane transport and cell-to-cell communication.

3.4 | *SnRK2.4* Mutation Reshapes the Proteome Upon 1 μM ABA Treatment

Comparative transcriptomic analysis of WT and *snrk2.4* genotypes exposed to 1 μM ABA revealed very similar GO terms (Tables S3.2, S3.5). In addition, the clade A *PP2C* genes showed a similar increase in expression in *snrk2.4* mutants compared to WT (Figure 4). Overall, the expression of only one gene (Table S3.7) was distinct between WT and *snrk2.4* genotypes exposed to ABA. Thus, as observed in standard conditions, SnRK2.4 has a negligible impact on gene expression upon ABA treatment.

At the proteome level, the abundance of 41 and 56 proteins was significantly decreased and increased, respectively, in *snrk2.4* plants treated with ABA when compared to WT plants under the same conditions (Tables S5.6 and S5.7). Thus, as compared to standard conditions, SnRK2.4 has a more pronounced effect on the proteome upon ABA treatment. The over-accumulated proteome in *snrk2.4* plants treated with ABA was enriched in RNA helicases (Table S5.7) (RH52, RH32, RCF1, RH7), the function of which is required for pre-mRNA maturation. Since the abundance of the corresponding transcripts was not altered in *snrk2.4* genotypes, we propose that the degradation of these helicases upon ABA treatment is post-translationally controlled by SnRK2.4.

3.5 | *SnRK2.4* Mutation Reshapes the Phosphoproteome Upon 1 μM ABA Treatment

When analyzed under ABA conditions, *snrk2.4* plants showed a massive decrease in phosphorylated proteins. Only 2 proteins (QUA2, AT1G78240, and SRF6 AT1G53730) showed a significant increase in phosphorylation (Table S6), whereas 332 phosphopeptides corresponding to 277 proteins showed a significant decrease in abundance in the *snrk2.4* compared to WT plants (Table S5.8). Most of the corresponding proteins (80%) did not show any variation in abundance (Table S4). Thus, the differences in phosphopeptide abundance observed between WT and *snrk2.4* were caused by a genuine difference

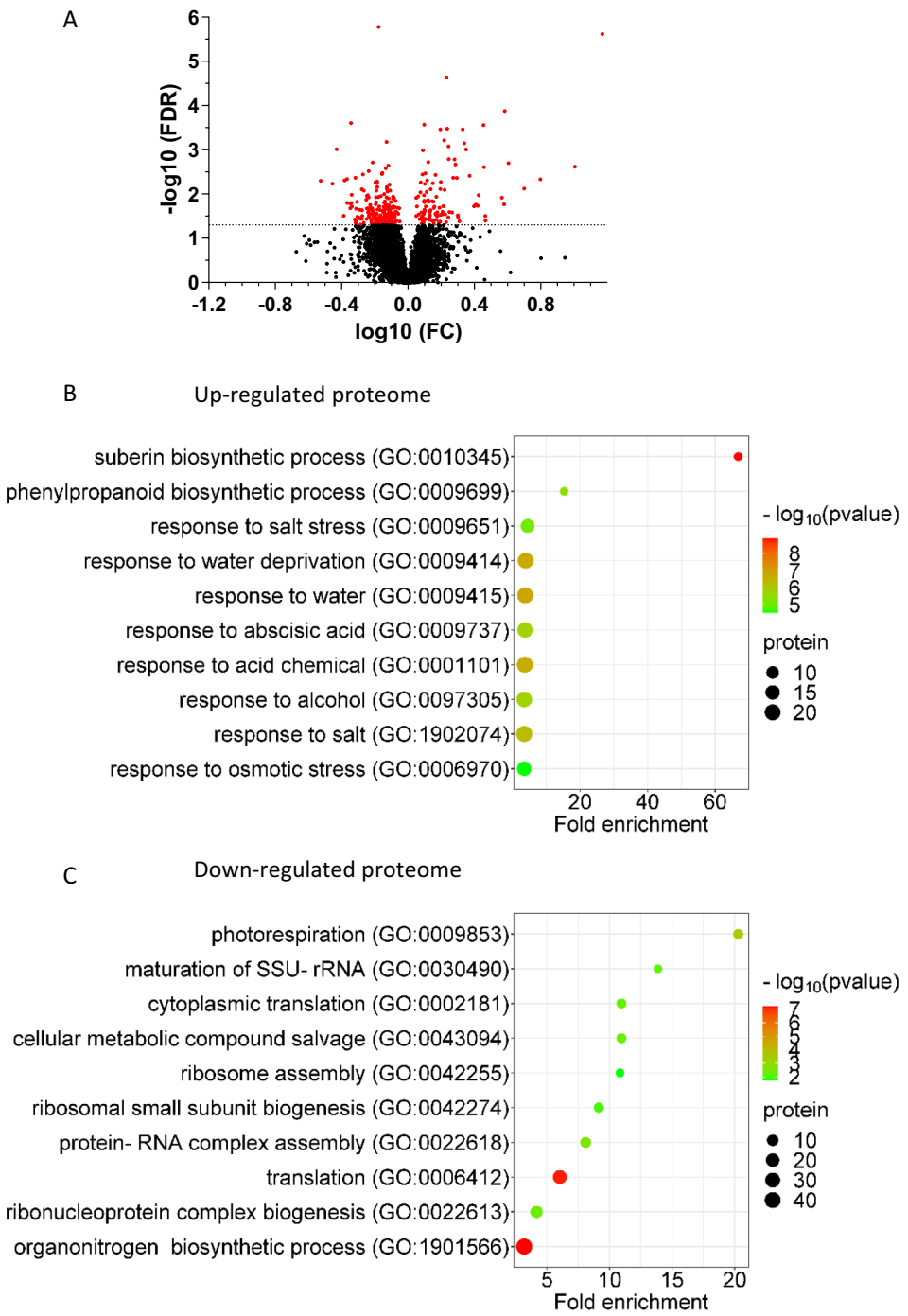

FIGURE 5 | Response of WT plant proteome to 1 μM ABA treatment for 3 h. (A) Volcano plot representing significant up- and down accumulated proteins in WT plants upon 1 μM ABA treatment. (B, C) Enriched biological process terms of up- (B) and down (C)-accumulated proteins. Significant corrected *p*-value and fold enrichment were below 10^{-3} and above 3, respectively. Proteins characterizing GO terms are described in Tables S5.1, S5.2.

in phosphorylation stoichiometry. Analysis of GO terms enrichment (Figure 9) showed that, upon ABA treatment, SnRK2.4 induced the phosphorylation of proteins involved in major membrane physiological processes: transmembrane transports (including nitrate, phosphate, sulfate, chloride, calcium, iron, potassium, magnesium, sodium, malate, and proton); cell wall biogenesis with 4 cellulose synthases; vesicle-mediated transport with a syntaxin (SYP122), 2 vesicle-associated proteins (PVA11, PVA12), a SNARE-interacting protein KEULE, and an exocyst component (SEC8); protein degradation to the vacuole with TOM1-LIKE proteins (TOL1, TOL2, TOL6); cell-to-cell communication with 44 proteins described at plasmodesmata. In addition, SnRK2.4 enhanced the ABA-dependent phosphorylation of 41 PKs belonging to the following PK families (Table S5.9): 7 CDPKs (CRK2, CPK6, CRK6, CPK9, CPK13, CPK29), 3 MAPKs (MAP4K4, MPK8, Raf15, ILK4 Raf-like protein), 18 receptor kinases, including leucine-rich RLK (LRR-RLK), and 3 AGC kinases (PDK1, IREH1, AT5G09890). These data indicate that

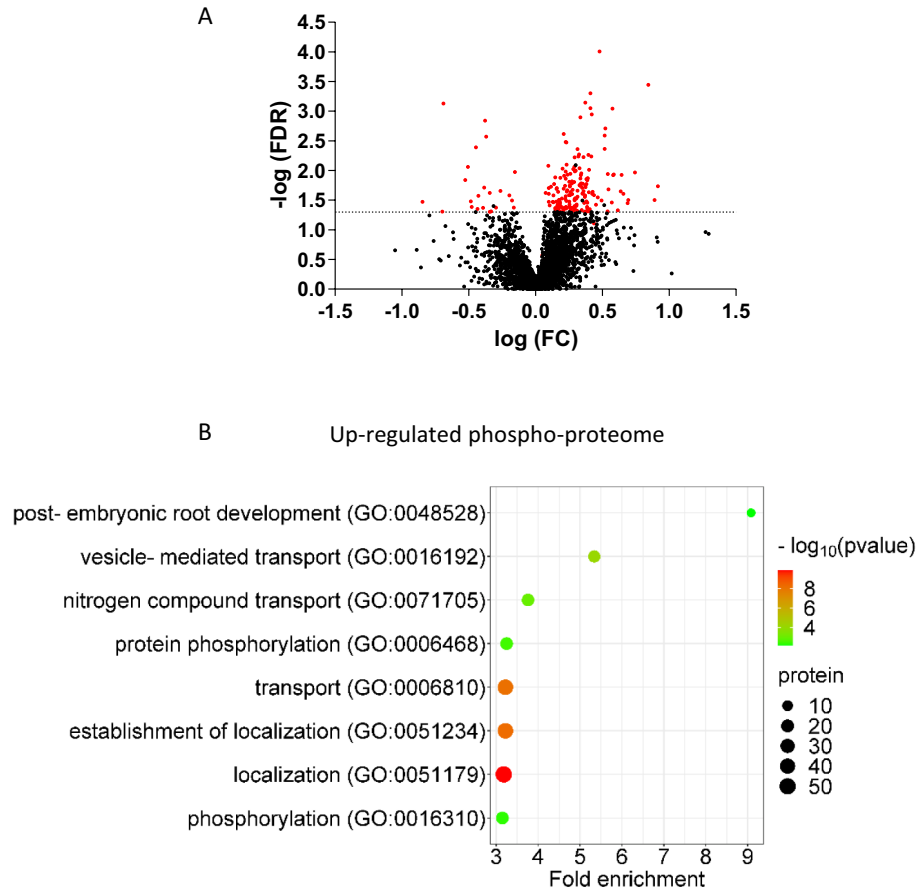

FIGURE 6 | Response of WT plant phospho-proteome to 1 μM ABA treatment for 3 h. (A) Volcano plot representing significant accumulated phospho-peptides in WT plant upon 1 μM ABA treatment. (B) Enriched biological process terms of accumulated phospho-proteins. Significant corrected *p*-value and fold enrichment were below 10^{-3} and above 3, respectively. Proteins characterizing GO terms are described in Table S5.3.

SnRK2.4 stimulation by ABA induces activation of a wider set of PKs than in standard conditions.

4 | Discussion

SnRK2.4 was originally described as an ABA-insensitive, osmotic, and salt stress-activated SnRK2 (Boudsocq et al. 2004; McLoughlin et al. 2012). Here, we show that SnRK2.4 has a residual activity under standard conditions and is further activated in response to ABA. Our findings are based on the detailed analysis of two allelic *snrk2.4* mutants, which provide two independent lines of evidence: a role for SnRK2.4 in lateral root growth and development, as revealed by root phenotyping, and the identification of several dozen downstream effector proteins of SnRK2.4 using a comparative phosphoproteomic approach.

4.1 | ABA-Dependent and Independent Effects of SnRK2.4 on Lateral Root Development

Two recent studies suggested a role for SnRK2.4 in ABA signaling (Ruschhaupt et al. 2019; Shahzad et al. 2024). Ruschhaupt et al. (2019) first showed that SnRK2.4 forms functionally active core ABA signaling complexes in combination with PYR/PYL receptors and PP2Cs co-receptors in yeast. Shahzad et al. 2024 investigated the role of SnRK2.4 in root hydraulics. Here, we investigated effects on root system architecture of low ABA concentrations (1–5 μM), taking as a reference a double mutant for well-established ABA-responsive SnRK2s, SnRK2.2 and SnRK2.3. A predominant role for at least one of these PKs in inhibition of primary root growth at 5 μM was observed (Figure 1A). We found that the reduction of lateral root and primordia densities at 1 μM ABA was mediated by SnRK2.4, whereas SnRK2.2 and/or SnRK2.3 contributed to an additional density reduction at a higher ABA concentration (5 μM) (Figure 1B). Thus, SnRK2s from different subclasses can mediate responses to exogenously applied ABA, but with distinct *in planta* hormone sensitivity. Here, SnRK2.4 showed a higher ABA sensitivity for lateral root development than the two canonical ABA-responsive SnRK2s. The high ABA sensitivity of SnRK2.4 seen here and after functional expression in yeast suggests that the contribution of SnRK2.4 to other ABA responses may have been missed using exogenous ABA treatments, as it was possibly masked by effects of endogenous ABA. In WT plants, we observed that 1 μM ABA decreased LR density and primordia density by 18% and 58%, respectively (Figures 1B and 2), without affecting primary root length (Figure 1A). By contrast, *snrk2.4* mutants showed in the same conditions 25% inhibition of primordia initiation and no inhibition of LR density. This indicates that SnRK2.4 mediates at least in part the effects of ABA on both primordia initiation and emergence.

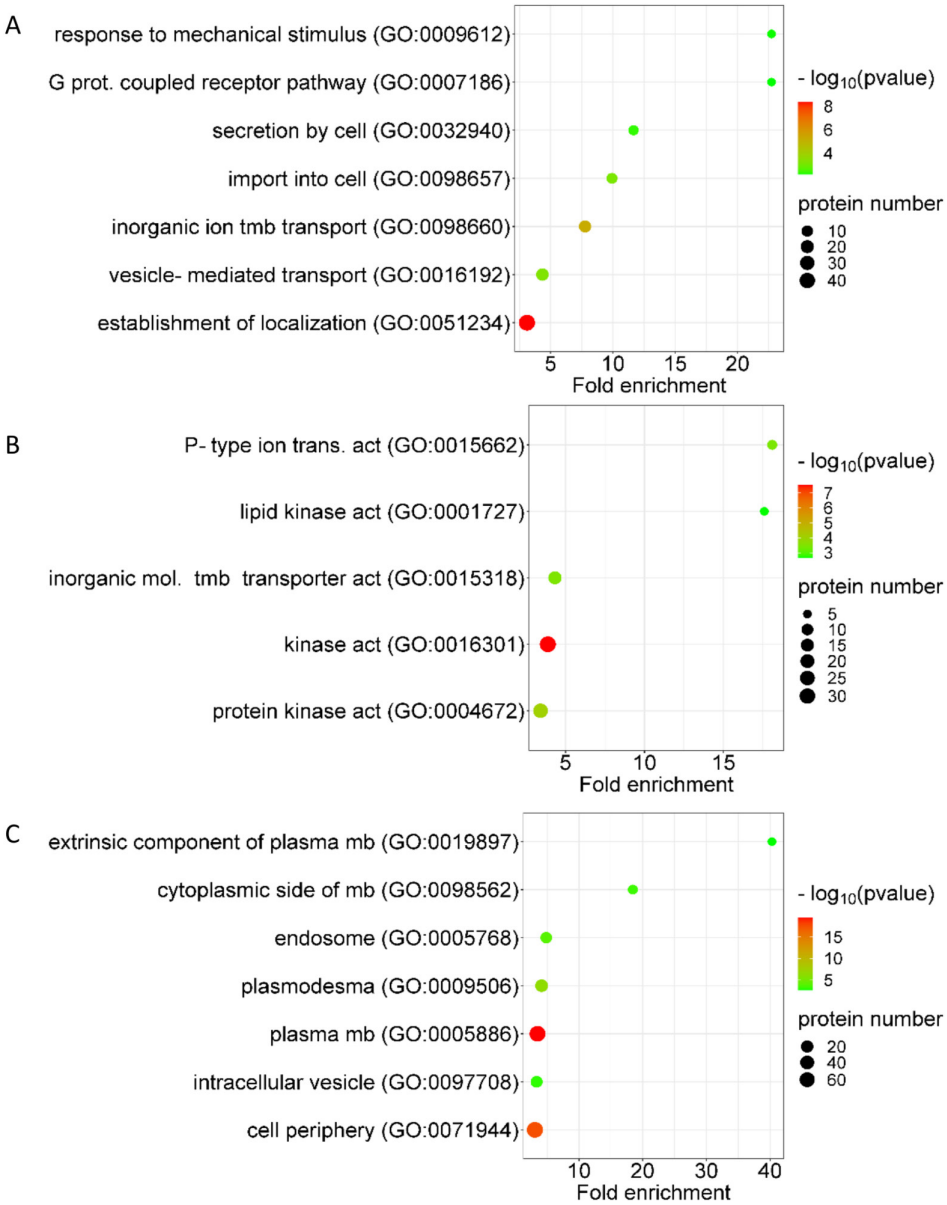

FIGURE 7 | Functional enrichment analysis of proteins, in standard conditions, and with decreased phosphorylation in *snrk2.4* mutants with respect to WT. (A) Biological process, (B) molecular function, (C) cellular component. Considered FDR and fold enrichment were below 10^{-3} and above 3, respectively. Numbers indicate the number of genes in each GO term. Proteins characterizing GO terms are described in Table S5.5. act, activity; mb, membrane; mol, molecular; tmb, transmembrane.

The *snrk2.4* mutants also showed alterations in lateral root and primordia densities in standard conditions (i.e., in the absence of exogenous ABA). These densities were lower in the mutants compared to WT (Figures 1 and 2), suggesting that SnRK2.4 positively contributes to lateral root formation in these conditions, highlighting a putative paradox in the function of SnRK2.4 with opposite effects between standard and ABA treatment conditions. We observed that 45% of proteins (82 proteins) with decreased phosphorylation in *snrk2.4* mutants in standard conditions were also under-phosphorylated in *snrk2.4* mutants under ABA (Tables S5.5, S5.8). Thus, in standard conditions, SnRK2.4 may be activated by either constitutive ABA-independent signal(s) or by low endogenous ABA levels.

A similar duality in functions has been previously reported for ABA-responsive class III SnRK2s (i.e., SnRK2.2 and SnRK2.3), which promote or repress root growth in standard and ABA conditions, respectively. This can be explained by the kinases' ability to sequester and inactivate the energy sensor SnRK1 in the absence of ABA (Belda-Palazón et al. 2020; Kamiyama, Katagiri, and Umezawa 2021). Noticeably, an interaction between SnRK2.4 and SnRK1 has been demonstrated *in planta* (Soma et al. 2020), suggesting that a similar sequestration and inactivation of SnRK1 by SnRK2.4 may occur.

4.2 | SnRK2.4 Contributes to PK-Mediated Phosphorylation Cascades

Besides root developmental phenotypes, marked changes in the proteome and phosphoproteome were induced by *snrk2.4* mutations, providing direct evidence for the molecular

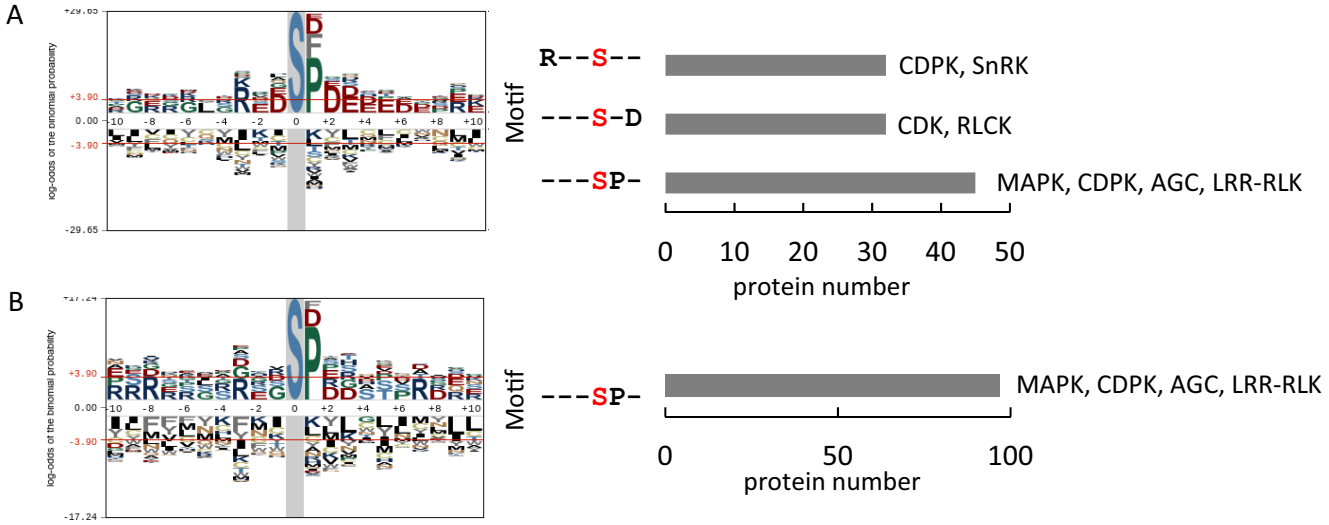

FIGURE 8 | Motif analysis of phosphorylated serine residues. Down-accumulated phospho-peptides in *snrk2.4* mutants in standard conditions (A) and in ABA conditions (B) were considered to determine motifs. The main P-logo motif, the statistically significant neighboring positions and the resulting motifs are shown. Putative protein kinases recognizing motifs are indicated. AGC, AGC kinase; CDK, ccyclin-dependent kinase; CDPK, ccalcium-dependent protein kinase; LRR-RLK, Lleucine-rich receptor-like kinase; MAPK, mmitogen-activated protein kinase; RLCK, rreceptor-like cytoplasmic kinase.

activity of SnRK2.4 *in planta*. In contrast, *SnRK2.4* knockout had a minor impact on the plant transcriptome. Such major decorrelation between gene expression and protein abundance suggests that SnRK2.4 mostly acts at the post-transcriptional level. Moreover, phosphoproteome analysis, substantiated by corresponding protein quantifications, indicated a net variation of phosphorylation for most identified proteins. Therefore, SnRK2.4-dependent responses, whether in standard conditions or under ABA treatment, are mostly exerted at the post-translational level.

One main reason is that SnRK2.4 seems to be involved in phosphorylation cascades involving multiple PKs. Thus, phosphorylation of 26 and 41 PKs, belonging to different PK families, was decreased in *snrk2.4* mutants in standard and ABA conditions, respectively (Table S5.9). Only 13 of them were altered in both conditions, showing a specific PK response according to each condition (i.e., standard and ABA). In both cases, we observed preferential targeting of a —SP— phosphorylation motif, which has been highlighted during ABA-mediated drought responses (Wong et al. 2019). This observation strengthens the link between SnRK2.4 function and ABA signaling. In addition, the —SP— motif is also recognized by other SnRK2s from subclass III (Umezawa et al. 2013), suggesting that this motif is characteristic of the whole SnRK2 family independently of the type of environmental stress. This motif is also a minimal MAPK target motif, suggesting an involvement of MAPK cascades in ABA signaling, as demonstrated in (Umezawa et al. 2013; Wang et al. 2013). More specifically, we observed that, under ABA treatment conditions, phosphorylation of several components of the MAPK family was dependent on SnRK2.4: MPK8, MAP4K4, and Raf-like protein kinase (Raf) 15 (Table S5.9). Raf are MAPKKKs classified into four B and seven C subgroups (Ichimura et al. 2002). Several studies have reported that group B Rafs regulate SnRK2s in *Arabidopsis* (Kamiyama, Katagiri, and Umezawa 2021; Lin et al. 2021; Soma et al. 2020; Takahashi et al. 2020). By contrast, group C Rafs, such as Raf36 and Raf22, were described as substrates of SnRK2s (Kamiyama, Hirotani, et al. 2021). In addition, Raf36 and Raf22 phosphorylation was shown to induce their degradation, thereby alleviating their ability to inhibit ABA signaling (Kamiyama, Hirotani, et al. 2021). According to these data, our results suggest that Raf15, unlike other group B Rafs, is a SnRK2.4 substrate and, similar to group C Rafs, may function as a negative regulator of ABA signaling.

In addition, 5 CPKs and two CRKs were underphosphorylated in their N-terminal (CPK6, CPK9, CRK2, CPK13) and C-terminal (CPK29, CRK6, and CPK13) regions in *snrk2.4* mutants upon ABA treatment (Table S4.9). The CRK family belongs to the Ser/Thr-type CDPK-sucrose non-fermenting-1-related PK superfamily (Hrabak et al. 2003). CDPKs act as signaling hubs in plant stress signaling and development (Schulz et al. 2013). CPKs and CRKs have sites that can be phosphorylated by themselves (auto-phosphorylation) or by upstream kinases, in a constitutive manner or after environmental stress stimulation (Schulz et al. 2013). Therefore, we suspect that some of these PKs are SnRK2.4 substrates in response to ABA.

4.3 | Molecular Targets of SnRK2.4

A recent phosphoproteomics study based on in vitro phosphorylation reactions using in vivo phosphorylated peptides as substrate pools to identify putative substrates of SnRK2.4 identified 67 proteins that are phosphorylated by SnRK2.4 in response to an osmotic treatment (Wang et al. 2020). These SnRK2.4 targets are different from the proteins identified in our work, suggesting a specificity of SnRK2.4 function, whether activated by an osmotic or an ABA stimulus. In addition, the discrepancy between the two studies can result from the different experimental setups, with the use of 10-day-old seedlings in (Wang et al. 2020) whereas our study deals with roots of 3-week-old plants. By contrast, a SnRK2.4 interactome, obtained from 3-week-old plants treated with mannitol, identified

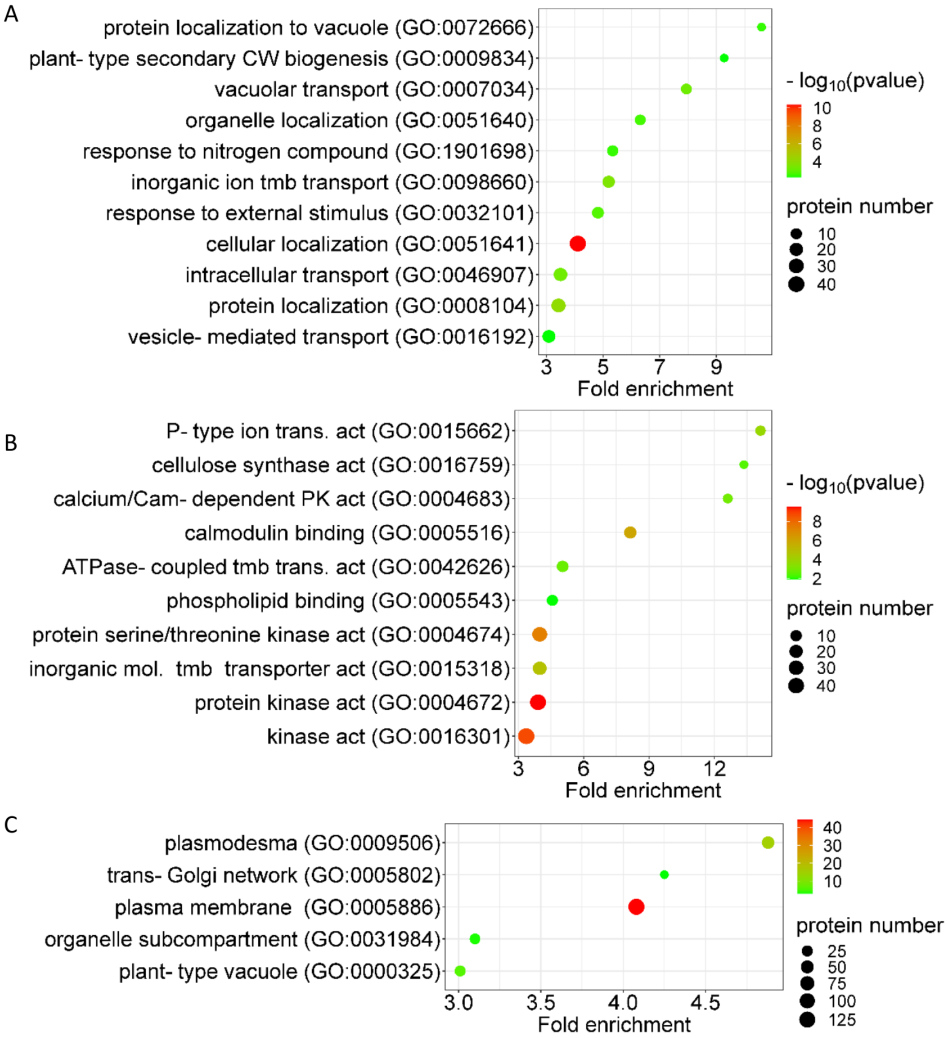

FIGURE 9 | Functional enrichment analysis of proteins, upon 1 μM ABA treatment, and with decreased phosphorylation in *snrk2.4* mutants with respect to the WT. (A) Biological process, (B) molecular function, (C) cellular component. Considered FDR and fold enrichment were below 10^{-3} and above 3, respectively. Numbers indicate the number of genes in each GO term. Proteins characterizing GO terms are described in Table S5.8. act., activity; Cam, calmodulin; CW, cell wall; mol, molecular; tmb, transmembrane.

1308 proteins that co-immunoprecipitate with SnRK2.4 (Soma et al. 2020). We noticed that 38 and 34 proteins were both identified in the SnRK2.4 interactome and under-phosphorylated in *snrk2.4* mutants, in ABA conditions and in standard conditions, respectively (Table S7). Thus, this analysis suggests that several under-phosphorylated proteins in *snrk2.4* mutants interact with SnRK2.4 and could be true SnRK2.4 substrates.

The first example of SnRK2.4 target uncovered in the present study is somewhat atypical as it indicates how the effects of SnRK2.4 on protein abundance may lead to altered gene expression. Hence, our work shows that SnRK2.4 induces the degradation of 4 DEAD box RNA helicases upon ABA (Table S4.7). The *Arabidopsis* genome contains 58 genes encoding such RNA helicases (Mingam et al. 2004), contributing to all aspects of RNA metabolism (Baek et al. 2018 for review), in particular during ABA and abiotic stress responses (Baek et al. 2018; Guan et al. 2013; Khan et al. 2014; Tuteja et al. 2013). Our results show that SnRK2.4 could downregulate RCF1 (AT1G20920, also called RH42) cellular abundance, an RNA helicase that maintains a correct splicing of pre-mRNAs of nuclear-encoded genes (Guan et al. 2013). SnRK2.1, a member of class I as SnRK2.4, was shown to interact with VARICOSE, an mRNA decapping activator, to decrease mRNA accumulation under osmotic stress conditions (Soma et al. 2017). Thus, class I SnRK2s appear as potential regulators of gene expression acting on mRNA splicing and stability.

We also found that phosphorylation of membrane transporters and components of membrane trafficking and cell-to-cell communication was altered by *SnRK2.4* mutation (Figures 7 and 9), with 25 and 44 proteins matching the GO term «plasmodesmata» in standard and ABA conditions, respectively (Tables S5.5, S5.8). Plasmodesmata are cytoplasmic channels that cross cell walls to allow cell-to-cell communication and can be modulated by callose deposition (Amsbury et al. 2018; Kitagawa et al. 2019). In this work, we observed that phosphorylation of a PM-located LRR-RLK, QSK1 (Qian Shou kinase, AT3G02880) at positions S621 and S626 was dependent on SnRK2.4 (Table S6). QSK1 phosphorylation at these sites was shown to regulate callose deposition at plasmodesmata and sites of lateral root formation during osmotic stress (Grison et al. 2019). Regulators of plasmodesmata function also

include members of the SnRK2 family: in *Physcomitrium patens*, an *At*SnRK2.6 orthologue, *Pp*SNRK2, was shown to be essential for ABA-induced closure of plasmodesmata (Tomoi et al. 2020). A recent work also revealed a role for SnRK2.2 in regulating plasmodesmata aperture during xerobranching (Mehra et al. 2022). Thus, we propose that SnRK2.4 and QSK1 could contribute to reducing cell-to-cell communication by enhancing callose deposition at plasmodesmata.

Within this work, we also identified three cellulose synthases (CESA1, CESA3, and CESA4) and one cellulose synthase-like D (CSLD3), the phosphorylation of which was dependent on SnRK2.4 (Table S5.8). The phosphorylation of CESAs influences the dynamics of the CESA complex (Li et al. 2025, Speicher et al. 2018 for review). Notably, phosphorylation of CESA3 at S211 (observed in our work) and at T212 has opposing effects on CESA3 activity (Chen et al. 2016). Constitutive phosphorylation of CESA1 at S688 (observed in our work) results in reduced cellulose induction and primary root length (Khan et al. 2024). A few PKs phosphorylating CESAs have been identified (Li et al. 2025), such as MAPKs (Boex-Fontvieille et al. 2014; Li et al. 2025; Wang et al. 2020), the brassinosteroid insensitive 2 (BIN2) (Sánchez-Rodríguez et al. 2017) and CPK32 (Xin et al. 2023). Here we propose that, upon ABA treatment, phosphorylation of CESA1, 3, and 4 depends on SnRK2.4, or on CDPKs and MAPKs activated by SnRK2.4. Such a cascade of PKs would alter CESA activity, leading to changes in LRd and primordium density by as yet unknown mechanisms.

Phosphorylation of three major enzymes that control the cellular amount of PtdIns(4,5)P_2 was decreased in *snrk2.4* mutants upon ABA treatment: the phosphatidylinositol 4-phosphate 5-kinase PIP5K7 that induces PtdIns(4,5)P_2 production, and the phospholipases C 2 (PLC2) and NPC3 that are involved in the consumption of PtdIns(4,5)P_2 (Table S6). PIP5K7 works as a key enzyme in PI signaling (Kuroda et al. 2021; Zhang et al. 2020) and PLC2 is the primary phospholipase in phosphoinositide metabolism (Kanehara et al. 2015). PLC2 functions in auxin-modulated root development in Arabidopsis (Chen, Li, et al. 2019) and an interaction between PLC-mediated signaling and ABA signaling was recently evidenced (Zhang et al. 2018). Moreover, the anionic phospholipid PA that rapidly accumulates in response to several stress conditions and represents an important signaling lipid in eukaryotes affects the localization and function of a diverse set of target proteins (Testerink and Munnik 2011), among which

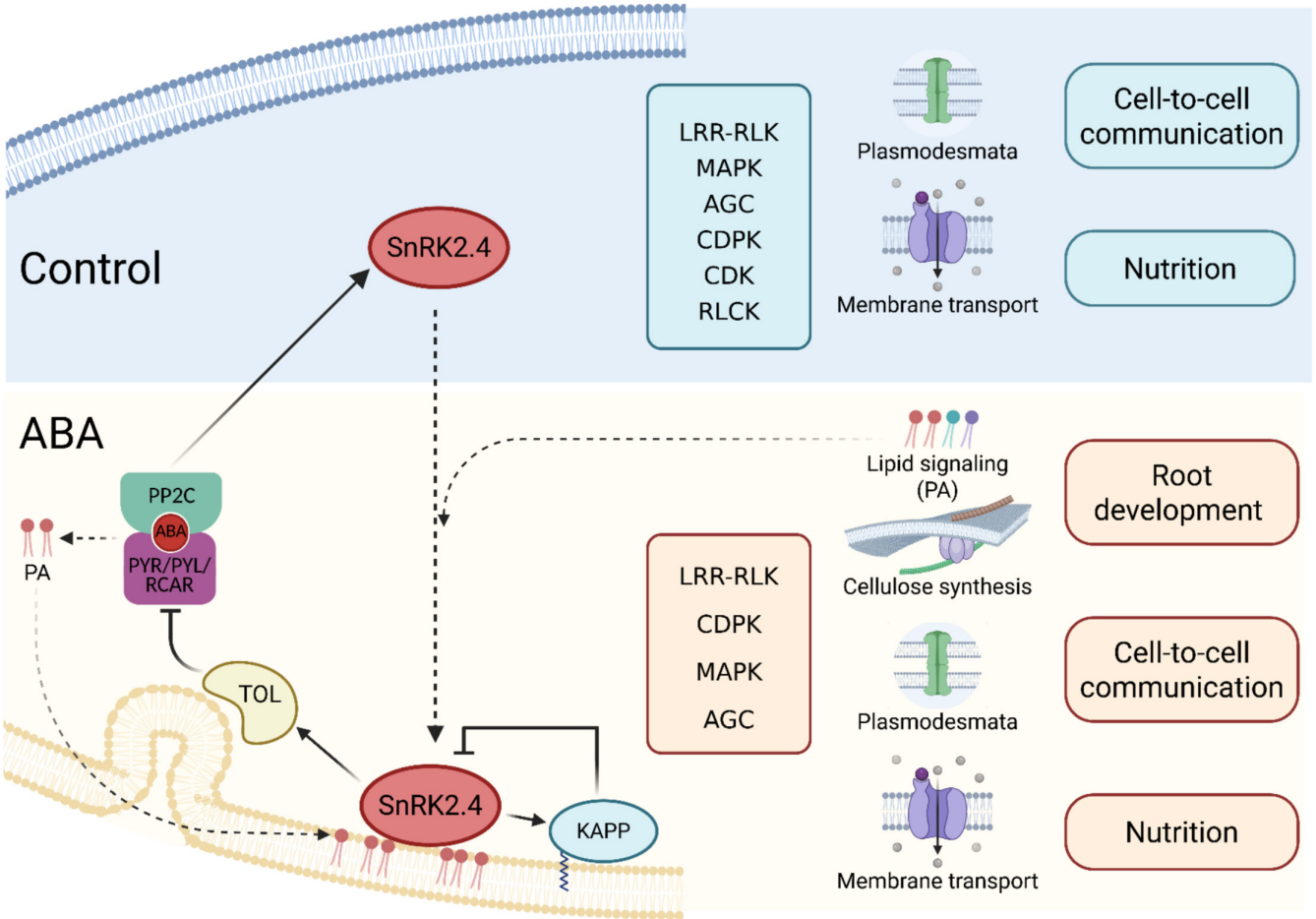

FIGURE 10 | Major pathways and targets regulated by SnRK2.4 under both standard and ABA treatment conditions. In standard conditions, SnRK2.4 targets membrane transport proteins and proteins involved in cell-to-cell communication, either by direct phosphorylation or indirectly via PK cascades. Under ABA treatment, an accumulation of PA is induced, which in turn triggers a re-localization of SnRK2.4 from the cytosol to the membrane (McLoughlin et al. 2012; Testerink et al. 2004). This mechanism would allow SnRK2.4 to target additional proteins controlling PI signaling and cellulose biosynthesis. The activation of KAPP and TOL by SnRK2.4-mediated phosphorylation could be involved in the attenuation of ABA signaling.

are several plant PKs, including SnRK2.4 (McLoughlin et al. 2012). Thus, we propose that PA, the accumulation of which is induced by ABA, binds to SnRK2.4 and induces its subcellular re-localization to membranes, thereby affecting SnRK2.4 interaction with direct phosphorylation targets. Overall, our data indicate that SnRK2.4 may interfere with lipid signaling in response to ABA, particularly during lateral root formation.

4.4 | Putative Attenuation of ABA Signaling by SnRK2.4

The attenuation of ABA signaling allows the plant to finely adapt to prolonged stressful conditions (Chen et al. 2020). The upregulation of clade A *PP2Cs* genes provides a negative feedback loop to desensitize ABA (Nakashima et al. 2009). While it has been shown to depend on subclass III SnRK2 (Nakashima et al. 2009), we show that it is independent of SnRK2.4 (Figure 4). By contrast, we observed upon ABA treatment a dephosphorylation of KAPP (AT5G19280) at S171 in *snrk2.4* mutants, while its phosphorylation increased by more than 2-fold in the WT plant (Table S6). By interacting with SnRK2.2, SnRK2.3, and SnRK2.6, KAPP was shown to negatively regulate ABA signaling (Lu et al. 2020). Its phosphorylation at S171 was reported in two studies (Nakagami et al. 2010; Umezawa et al. 2013) but its functional significance has remained elusive. Here, we propose that activation of KAPP by SnRK2.4-mediated phosphorylation could be involved in the attenuation of ABA signaling.

Another mechanism to attenuate ABA signaling is to degrade ABA receptors in the vacuole via the Endosomal Sorting Complex Required for Transport (ESCRT) machinery (Belda-Palazon et al. 2016; García-León et al. 2019). TOLs are ubiquitin receptors that target ubiquitinated cargoes for degradation to the ESCRT machinery. TOLS were recently shown to attenuate ABA signaling through degradation of ubiquitinated ABA receptors and transporters (Moulinier-Anzola et al. 2024). We observed that the phosphorylation of TOL1 at S33 or S35, TOL3 at S284 or S294, and TOL6 at S357 or S358 was decreased in *snrk2.4* mutants upon ABA (Table S6). Although the functional role of TOL phosphorylation is still elusive, we propose that SnRK2.4 could contribute to attenuate ABA signaling by phosphorylating and activating TOLs.

In conclusion, we show that SnRK2.4 is an ABA-responsive PK that contributes to the modulation of cell-to-cell communication, mRNA splicing, cellulose biosynthesis, and lipid signaling (Figure 10) via a complex PKs cascade. How these processes link SnRK2.4-mediated developmental responses, such as root meristem emergence and LR density, remains to be elucidated. Nevertheless, this work provides new avenues to explore the multiple roles of SnRK2.4 under resting conditions or after ABA stimulation.

Author Contributions

M.A. obtained protein material, performed proteomics experiments. C.T.-R. performed Q-RT PCR. experiments. V.R. conducted mass spectrometry experiments. P.N. supervised root phenotyping. V.D. performed statistical analysis of proteomic data. A.C. obtained root imaging. V.S. and C.M. conceived the study. V.S. supervised proteomics. V.S., C.M., and M.A. wrote the manuscript. All the authors have read and approved the final manuscript.

Acknowledgments

We thank Cécile Fizames and Sandrine Ruffel for help in the statistical analysis of root phenotyping data and microarray analysis, respectively. Mass spectrometry experiments were carried out using the facilities of the Montpellier Proteomics Platform (PPM, MSPP site BioCampus Montpellier), a member of the national Proteomics French Infrastructure (ProFI UAR 2048) supported by the French National Research Agency (ANR-24-INBS-0015, Investments for the future F2030).

Conflicts of Interest

The authors declare no conflicts of interest.

Data Availability Statement

All data can be found within the manuscript, in its supporting materials, and in ProteomeXchange consortium concerning raw proteomics data and at EBI concerning raw transcriptomics data.

References

Amsbury, S., P. Kirk, and Y. Benitez-Alfonso. 2018. "Emerging Models on the Regulation of Intercellular Transport by Plasmodesmata-Associated Callose." *Journal of Experimental Botany* 69: 105–115.

Baek, W., C. W. Lim, and S. C. Lee. 2018. "A DEAD-Box RNA Helicase, RH8, Is Critical for Regulation of ABA Signalling and the Drought Stress Response via Inhibition of PP2CA Activity." *Plant, Cell & Environment* 41: 1593–1604.

Belda-Palazon, B., L. Rodriguez, M. A. Fernandez, et al. 2016. "FYVE1/FREE1 Interacts With the PYL4 ABA Receptor and Mediates Its Delivery to the Vacuolar Degradation Pathway." *Plant Cell* 28: 2291–2311.

Belda-Palazón, B., M. Adamo, C. Valerio, et al. 2020. "A Dual Function of SnRK2 Kinases in the Regulation of SnRK1 and Plant Growth." *Nature Plants* 6: 1345–1353.

Berger, N., V. Demolombe, S. Hem, et al. 2022. "Root Membrane Ubiquitinome Under Short-Term Osmotic Stress." *International Journal of Molecular Sciences* 23: 1956.

Boex-Fontvieille, E., M. Davanture, M. Jossier, M. Zivy, M. Hodges, and G. Tcherkez. 2014. "Photosynthetic Activity Influences Cellulose Biosynthesis and Phosphorylation of Proteins Involved Therein in Arabidopsis Leaves." *Journal of Experimental Botany* 65: 4997–5010.

Boudsocq, M., H. Barbier-Brygoo, and C. Laurière. 2004. "Identification of Nine Sucrose Nonfermenting 1-Related Protein Kinases 2 Activated by Hyperosmotic and Saline Stresses in *Arabidopsis thaliana*." *Journal of Biological Chemistry* 279: 41758–41766.

Brandt, B., S. Munemasa, C. Wang, et al. 2015. "Calcium Specificity Signaling Mechanisms in Abscisic Acid Signal Transduction in *Arabidopsis* Guard Cells." *eLife* 4: e03599.

Casimiro, I., T. Beeckman, N. Graham, et al. 2003. "Dissecting Arabidopsis Lateral Root Development." *Trends in Plant Science* 8: 165–171.

Chen, K., G. J. Li, R. A. Bressan, C. P. Song, J. K. Zhu, and Y. Zhao. 2020. "Abscisic Acid Dynamics, Signaling, and Functions in Plants." *Journal of Integrative Plant Biology* 62: 25–54.

Chen, S. L., H. L. Jia, H. Y. Zhao, et al. 2016. "Anisotropic Cell Expansion Is Affected Through the Bidirectional Mobility of Cellulose Synthase Complexes and Phosphorylation at Two Critical Residues on CESA3." *Plant Physiology* 171: 242–250.

Chen, X., L. Li, B. X. Xu, et al. 2019. "Phosphatidylinositol-Specific Phospholipase C2 Functions in Auxin-Modulated Root Development." *Plant, Cell & Environment* 42: 1441–1457.

Chen, Y., V. Rofidal, S. Hem, et al. 2019. "Targeted Proteomics Allows Quantification of Ethylene Receptors and Reveals SIETR3 Accumulation in Never-Ripe Tomatoes." *Frontiers in Plant Science* 10: 1054.

Cutler, S. R., P. L. Rodriguez, R. R. Finkelstein, and S. R. Abrams. 2010. "Abscisic Acid: Emergence of a Core Signaling Network." In *Annual Review of Plant Biology*, edited by S. Merchant, W. R. Briggs, and D. Ort, vol. 61, 651–679. Annual Reviews.

Czechowski, T., M. Stitt, T. Altmann, M. K. Udvardi, and W. R. Scheible. 2005. "Genome-Wide Identification and Testing of Superior Reference Genes for Transcript Normalization in Arabidopsis." *Plant Physiology* 139: 5–17.

De Smet, I., L. Signora, T. Beeckman, D. Inzé, C. H. Foyer, and H. M. Zhang. 2003. "An Abscisic Acid-Sensitive Checkpoint in Lateral Root Development of *Arabidopsis*." *Plant Journal* 33: 543–555.

Di Pietro, M., J. Vialaret, G.-W. Li, et al. 2013. "Coordinated Post-Translational Responses of Aquaporins to Abiotic and Nutritional Stimuli in *Arabidopsis* Roots." *Molecular and Cellular Proteomics* 12: 3886–3897.

Diaz, M., M. J. Sanchez-Barrena, J. M. Gonzalez-Rubio, et al. 2016. "Calcium-Dependent Oligomerization of CAR Proteins at Cell Membrane Modulates ABA Signaling." *Proceedings of the National Academy of Sciences of the United States of America* 113: E396–E405.

Dietrich, D., L. Pang, A. Kobayashi, et al. 2017. "Root Hydrotropism Is Controlled via a Cortex-Specific Growth Mechanism." *Nature Plants* 3: 17057.

Edel, K. H., and J. Kudla. 2016. "Integration of Calcium and ABA Signaling." *Current Opinion in Plant Biology* 33: 83–91.

El-Khatib, R. T., A. G. Good, and D. G. Muench. 2007. "Analysis of the Arabidopsis Cell Suspension Phosphoproteome in Response to Short-Term Low Temperature and Abscisic Acid Treatment." *Physiologia Plantarum* 129: 687–697.

Fàbregas, N., T. Yoshida, and A. R. Fernie. 2020. "Role of Raf-Like Kinases in SnRK2 Activation and Osmotic Stress Response in Plants." *Nature Communications* 11: 6184.

Fuchs, S., E. Grill, I. Meskiene, and A. Schweighofer. 2013. "Type 2C Protein Phosphatases in Plants." *FEBS Journal* 280: 681–693.

Fujii, H., P. E. Verslues, and J. K. Zhu. 2011. "Arabidopsis Decuple Mutant Reveals the Importance of SnRK2 Kinases in Osmotic Stress Responses In Vivo." *Proceedings of the National Academy of Sciences of the United States of America* 108: 1717–1722.

Fujii, H., and J. K. Zhu. 2009. "Arabidopsis Mutant Deficient in 3 Abscisic Acid-Activated Protein Kinases Reveals Critical Roles in Growth, Reproduction, and Stress." *Proceedings of the National Academy of Sciences of the United States of America* 106: 8380–8385.

García-León, M., L. Cuyas, D. Abd El-Moneim, et al. 2019. "Arabidopsis ALIX Regulates Stomatal Aperture and Turnover of Abscisic Acid Receptors." *Plant Cell* 31: 2411–2429.

Grison, M. S., P. Kirk, M. L. Brault, et al. 2019. "Plasma Membrane-Associated Receptor-Like Kinases Relocalize to Plasmodesmata in Response to Osmotic Stress." *Plant Physiology* 181: 142–160.

Guan, Q. M., J. M. Wu, Y. Y. Zhang, et al. 2013. "A DEAD Box RNA Helicase Is Critical for Pre-mRNA Splicing, Cold-Responsive Gene Regulation, and Cold Tolerance in *Arabidopsis*." *Plant Cell* 25: 342–356.

Guo, J. J., S. C. Wang, O. Valerius, et al. 2011. "Involvement of Arabidopsis RACK1 in Protein Translation and Its Regulation by Abscisic Acid." *Plant Physiology* 155: 370–383.

Hrabak, E. M., C. W. M. Chan, M. Gribskov, et al. 2003. "The Arabidopsis CDPK-SnRK Superfamily of Protein Kinases." *Plant Physiology* 132: 666–680.

Ichimura, K., K. Shinozaki, G. Tena, et al. 2002. "Mitogen-Activated Protein Kinase Cascades in Plants: A New Nomenclature." *Trends in Plant Science* 7: 301–308.

Kamiyama, Y., M. Hirotani, S. Ishikawa, et al. 2021. "*Arabidopsis* Group C Raf-Like Protein Kinases Negatively Regulate Abscisic Acid Signaling and Are Direct Substrates of SnRK2." *Proceedings of the National Academy of Sciences of the United States of America* 118: e2100073118.

Kamiyama, Y., S. Katagiri, and T. Umezawa. 2021. "Growth Promotion or Osmotic Stress Response: How SNF1-Related Protein Kinase 2 (SnRK2) Kinases Are Activated and Manage Intracellular Signaling in Plants." *Plants* 10: 1443.

Kanehara, K., C. Y. Yu, Y. Cho, et al. 2015. "Arabidopsis AtPLC2 Is a Primary Phosphoinositide-Specific Phospholipase C in Phosphoinositide Metabolism and the Endoplasmic Reticulum Stress Response." *PLoS Genetics* 11: e1005511.

Kawa, D., A. J. Meyer, H. L. Dekker, et al. 2020. "SnRK2 Protein Kinases and mRNA Decapping Machinery Control Root Development and Response to Salt." *Plant Physiology* 182: 361–377.

Khan, A., A. Garbelli, S. Grossi, et al. 2014. "The Arabidopsis STRESS RESPONSE SUPPRESSOR DEAD-Box RNA Helicases Are Nucleolar- and Chromocenter-Localized Proteins That Undergo Stress-Mediated Relocalization and Are Involved in Epigenetic Gene Silencing." *Plant Journal* 79: 28–43.

Khan, G. A., A. Dutta, A. van de Meene, et al. 2024. "Phosphate Starvation Regulates Cellulose Synthesis to Modify Root Growth." *Plant Physiology* 194: 1204–1217.

Kitagawa, M., T. Tomoi, T. Fukushima, et al. 2019. "Abscisic Acid Acts as a Regulator of Molecular Trafficking Through Plasmodesmata in the Moss *Physcomitrella patens*." *Plant and Cell Physiology* 60: 738–751.

Kline, K. G., G. A. Barrett-Wilt, and M. R. Sussman. 2010. "In Planta Changes in Protein Phosphorylation Induced by the Plant Hormone Abscisic Acid." *Proceedings of the National Academy of Sciences of the United States of America* 36: 15986–15991.

Kulik, A., I. Wawer, E. Krzywinska, M. Bucholc, and G. Dobrowolska. 2011. "SnRK2 Protein Kinases-Key Regulators of Plant Response to Abiotic Stresses." *Omics-a Journal of Integrative Biology* 15: 859–872.

Kuroda, R., M. Kato, T. Tsuge, and T. Aoyama. 2021. "Arabidopsis Phosphatidylinositol 4-Phosphate 5-Kinase Genes *PIP5K7*, *PIP5K8*, and *PIP5K9* Are Redundantly Involved in Root Growth Adaptation to Osmotic Stress." *Plant Journal* 106: 913–927.

Li, W., J. Wei, Y. Lei, et al. 2025. "Phosphorylation of Cellulose Synthases in Plant Responses to Environmental Changes." *International Journal of Biological Macromolecules* 292: 139313.

Lin, Z., Y. Li, Y. B. Wang, et al. 2021. "Initiation and Amplification of SnRK2 Activation in Abscisic Acid Signaling." *Nature Communications* 12: 2456.

Lu, K., Y. D. Zhang, C. F. Zhao, et al. 2020. "The Arabidopsis Kinase-Associated Protein Phosphatase KAPP, Interacting With Protein Kinases SnRK2.2/2.3/2.6, Negatively Regulates Abscisic Acid Signaling." *Plant Molecular Biology* 102: 199–212.

McLoughlin, F., C. S. Galvan-Ampudia, M. M. Julkowska, et al. 2012. "The Snf1-Related Protein Kinases SnRK2.4 and SnRK2.10 Are Involved in Maintenance of Root System Architecture During Salt Stress." *Plant Journal* 72: 436–449.

Mehra, P., B. K. Pandey, D. Melebari, et al. 2022. "Hydraulic Flux-Responsive Hormone Redistribution Determines Root Branching." *Science* 378: 762–768.

Mi, H. Y., A. Muruganujan, J. T. Casagrande, and P. D. Thomas. 2013. "Large-Scale Gene Function Analysis With the PANTHER Classification System." *Nature Protocols* 8: 1551–1566.

Miao, R., W. Yuan, Y. Wang, et al. 2021. "Low ABA Concentration Promotes Root Growth and Hydrotropism Through Relief of ABA INSENSITIVE 1-Mediated Inhibition of Plasma Membrane H^+-ATPase 2." *Science Advances* 7: eabd4113.

Mingam, A., C. Toffano-Nioche, V. Brunaud, N. Boudet, M. Kreis, and A. Lecharny. 2004. "DEAD-Box RNA Helicases in *Arabidopsis thaliana*: Establishing a Link Between Quantitative Expression, Gene Structure and Evolution of a Family of Genes." *Plant Biotechnology Journal* 2: 401–415.

Moulinier-Anzola, J., M. Schwihla, R. Lugsteiner, et al. 2024. "Modulation of Abscisic Acid Signaling via Endosomal TOL Proteins." *New Phytologist* 243: 1065–1081.

Murashige, T., and F. Skoog. 1962. "A Revised Medium for Rapid Growth and Bioassays With Tobacco Tissue Cultures." *Physiologia Plantarum* 15: 473–497.

Nakagami, H., N. Sugiyama, K. Mochida, et al. 2010. "Large-Scale Comparative Phosphoproteomics Identifies Conserved Phosphorylation Sites in Plants." *Plant Physiology* 153: 1161–1174.

Nakashima, K., Y. Fujita, N. Kanamori, et al. 2009. "Three Arabidopsis SnRK2 Protein Kinases, SRK2D/SnRK2.2, SRK2E/SnRK2.6/OST1 and SRK2I/SnRK2.3, Involved in ABA Signaling Are Essential for the Control of Seed Development and Dormancy." *Plant and Cell Physiology* 50: 1345–1363.

Ruschhaupt, M., J. Mergner, S. Mucha, et al. 2019. "Rebuilding Core Abscisic Acid Signaling Pathways of Arabidopsis in Yeast." *EMBO Journal* 38: e101859.

Sánchez-Rodríguez, C., K. Ketelaar, R. Schneider, et al. 2017. "BRASSINOSTEROID INSENSITIVE2 Negatively Regulates Cellulose Synthesis in *Arabidopsis* by Phosphorylating Cellulose Synthase 1." *Proceedings of the National Academy of Sciences of the United States of America* 114: 3533–3538.

Schneider, C. A., W. S. Rasband, and K. W. Eliceiri. 2012. "NIH Image to ImageJ: 25 Years of Image Analysis." *Nature Methods* 9: 671–675.

Schulz, P., M. Herde, and T. Romeis. 2013. "Calcium-Dependent Protein Kinases: Hubs in Plant Stress Signaling and Development." *Plant Physiology* 163: 523–530.

Schweighofer, A., H. Hirt, and L. Meskiene. 2004. "Plant PP2C Phosphatases: Emerging Functions in Stress Signaling." *Trends in Plant Science* 9: 236–243.

Shahzad, Z., M. Canut, C. Tournaire-Roux, et al. 2016. "A Potassium-Dependent Oxygen Sensing Pathway Regulates Plant Root Hydraulics." *Cell* 167: 87–98.

Shahzad, Z., C. Tournaire-Roux, M. Canut, et al. 2024. "Protein Kinase SnRK2.4 Is a Key Regulator of Aquaporins and Root Hydraulics in Arabidopsis." *Plant Journal* 117: 264–279.

Soma, F., J. Mogami, T. Yoshida, et al. 2017. "ABA-Unresponsive SnRK2 Protein Kinases Regulate mRNA Decay Under Osmotic Stress in Plants." *Nature Plants* 3: 16204.

Soma, F., F. Takahashi, T. Suzuki, K. Shinozaki, and K. Yamaguchi-Shinozaki. 2020. "Plant Raf-Like Kinases Regulate the mRNA Population Upstream of ABA-Unresponsive SnRK2 Kinases Under Drought Stress." *Nature Communications* 11: 1373.

Soma, F., F. Takahashi, K. Yamaguchi-Shinozaki, and K. Shinozaki. 2021. "Cellular Phosphorylation Signaling and Gene Expression in Drought Stress Responses: ABA-Dependent and ABA-Independent Regulatory Systems." *Plants* 10: 756.

Soon, F. F., L. M. Ng, X. E. Zhou, et al. 2012. "Molecular Mimicry Regulates ABA Signaling by SnRK2 Kinases and PP2C Phosphatases." *Science* 335: 85–88.

Speicher, T. L., P. Z. Q. Li, and I. S. Wallace. 2018. "Phosphoregulation of the Plant Cellulose Synthase Complex and Cellulose Synthase-Like Proteins." *Plants* 7: 52.

Takahashi, Y., J. B. Zhang, P. K. Hsu, et al. 2020. "MAP3Kinase-Dependent SnRK2-Kinase Activation Is Required for Abscisic Acid Signal Transduction and Rapid Osmotic Stress Response." *Nature Communications* 11: 12.

Testerink, C., H. L. Dekker, Z. Y. Lim, et al. 2004. "Isolation and Identification of Phosphatidic Acid Targets from Plants." *Plant Journal* 39: 527–536.

Testerink, C., and T. Munnik. 2011. "Molecular, Cellular, and Physiological Responses to Phosphatidic Acid Formation in Plants." *Journal of Experimental Botany* 62: 2349–2361.

Tomoi, T., K. Kawade, M. Kitagawa, Y. Sakata, H. Tsukaya, and T. Fujita. 2020. "Quantitative Imaging Reveals Distinct Contributions of SnRK2 and ABI3 in Plasmodesmatal Permeability in *Physcomitrella patens*." *Plant and Cell Physiology* 61: 942–956.

Tuteja, N., R. K. Sahoo, B. Garg, and R. Tuteja. 2013. "OsSUV3 Dual Helicase Functions in Salinity Stress Tolerance by Maintaining Photosynthesis and Antioxidant Machinery in Rice (*Oryza sativa* L. cv. IR64)." *Plant Journal* 76: 115–127.

Umezawa, T., N. Sugiyama, F. Takahashi, et al. 2013. "Genetics and Phosphoproteomics Reveal a Protein Phosphorylation Network in the Abscisic Acid Signaling Pathway in *Arabidopsis thaliana*." *Science Signaling* 6: rs8.

Wang, P. C., C. C. Hsu, Y. Y. Du, et al. 2020. "Mapping Proteome-Wide Targets of Protein Kinases in Plant Stress Responses." *Proceedings of the National Academy of Sciences of the United States of America* 117: 3270–3280.

Wang, P. C., L. Xue, G. Batelli, et al. 2013. "Quantitative Phosphoproteomics Identifies SnRK2 Protein Kinase Substrates and Reveals the Effectors of Abscisic Acid Action." *Proceedings of the National Academy of Sciences of the United States of America* 110: 11205–11210.

Wong, M. M., G. B. Bhaskara, T. N. Wen, et al. 2019. "Phosphoproteomics of Arabidopsis Highly ABA-Induced1 Identifies AT-Hook-Like10 Phosphorylation Required for Stress Growth Regulation." *Proceedings of the National Academy of Sciences of the United States of America* 116: 2354–2363.

Wu, R. H., N. Dephoure, W. Haas, et al. 2011. "Correct Interpretation of Comprehensive Phosphorylation Dynamics Requires Normalization by Protein Expression Changes." *Molecular & Cellular Proteomics* 10, no. 8: 1–12.

Xin, X. R., D. H. Wei, L. Lei, et al. 2023. "CALCIUM-DEPENDENT PROTEIN KINASE32 Regulates Cellulose Biosynthesis Through Post-Translational Modification of Cellulose Synthase." *New Phytologist* 239: 2212–2224.

You, Z., S. Y. Guo, Q. Li, et al. 2023. "The CBL1/9-CIPK1 Calcium Sensor Negatively Regulates Drought Stress by Phosphorylating the PYLs ABA Receptor." *Nature Communications* 14: 5886.

Zhang, Q., R. van Wijk, M. Shahbaz, et al. 2018. "Arabidopsis Phospholipase C3 Is Involved in Lateral Root Initiation and ABA Responses in Seed Germination and Stomatal Closure." *Plant and Cell Physiology* 59: 469–486.

Zhang, Z. B., Y. T. Li, K. Huang, W. W. Xu, C. Zhang, and H. Y. Yuan. 2020. "Genome-Wide Systematic Characterization and Expression Analysis of the Phosphatidylinositol 4-Phosphate 5-Kinases in Plants." *Gene* 756: 144915.

Zhu, F. Y., M. X. Chen, N. H. Ye, et al. 2017. "Proteogenomic Analysis Reveals Alternative Splicing and Translation as Part of the Abscisic Acid Response in Arabidopsis Seedlings." *Plant Journal* 91: 518–533.

Supporting Information

Additional supporting information can be found online in the Supporting Information section. **Figure S1:** Effect of data normalization (A, B) and principal component analysis (C, D) of proteomic (A, C) and phospho-proteomic (B, D) data. For total proteome quantification, peptide ion intensity values derived from MaxQuant were subjected for label-free quantitation. To normalize phosphoproteomics samples, the intensity of each peptide from the "evidence" table was reported to the sum of all peptides intensity in each sample. **Figure S2:** schematic representation of the OMIC's experimental workflow to identify downstream targets of SnRK2.4. The transcriptome, proteome and phosphoproteome of WT plants and of two independent *snrk2.4* mutants treated or not with 1 μM ABA, were analyzed. Transcriptome was obtained with the GeneChipWT PLUS Reagent kit (Affymetrix). Phosphopeptides were enriched using titanium columns. Database searches were carried out using MaxQuant. Relative quantification was carried out using MaxQuant followed by statistical analysis of quantitative data to highlight proteins and phosphopeptides whose abundance was significantly modulated. The proportion of phosphorylated S, T, and Y residues is shown. **Figure S3:** typical pictures of MS plates with 15 days-old seedlings of Col, *snrk2.4–1*, *snrk4.2–2* and *snrk2.2x2.3* plants, cultivated in standard conditions and after transferring on 1 and 5 μM ABA. **Table S1:** primers used in the study. **Table S2:** number of lateral roots and primordia, in Col and in both *snrk2.4* mutants, measured within the same experiment. **Table S3:** gene expression in WT plant and *snrk2.4* mutants, in standard condition and after treatment with 1 μM ABA for 3 h. **Table S4:** identification and quantification of proteins in WT plant and *snrk2.4* mutants, in standard condition and after treatment with 1 μM ABA for 3 h. **Table S5:** Functional enrichment analyses of proteins and phosphoproteins exhibiting significant changes in abundance and in phosphorylation level, in WT plants and in *snrk2.4* mutants, in standard conditions and after treatment with 1 μM ABA for 3 h. **Table S6:** identification and quantification of phosphopeptides in the WT plant and in snrk2.4 mutants, in standard condition and after treatment with 1 μM ABA for 3 h. **Table S7:** SnRK2.4 interactors identified in (Soma et al. 2020) and identified in the present study as under-phosphorylated in *snrk2.4* mutants.